JOURNAL OF GEOPHYSICAL RESEARCH, VOL. 113, G00B08, doi: 10.1029/2007JG000592, 2008

Dynamics of carbon, biomass, and structure in two Amazonian forests

Elizabeth Hammond Pyle,[1] Gregory W. Santoni,[1] Henrique E. M. Nascimento,[2] Lucy R. Hutyra,[1,3] Simone Vieira,[4] Daniel J. Curran,[1] Joost van Haren,[5] Scott R. Saleska,[5] V. Y. Chow,[1] Plinio B. Carmago,[4] William F. Laurance,[2,6] and Steven C. Wofsy[1]

Received 13 September 2007; revised 23 July 2008; accepted 5 August 2008; published 14 November 2008.

[1] Amazon forests are potentially globally significant sources or sinks for atmospheric carbon dioxide. In this study, we characterize the spatial trends in carbon storage and fluxes in both live and dead biomass (necromass) in two Amazonian forests, the Biological Dynamic of Forest Fragments Project (BDFFP), near Manaus, Amazonas, and the Tapajós National Forest (TNF) near Santarém, Pará. We assessed coarse woody debris (CWD) stocks, tree growth, mortality, and recruitment in ground-based plots distributed across the terra firme forest at both sites. Carbon dynamics were similar within each site, but differed significantly between the sites. The BDFFP and the TNF held comparable live biomass (167 ± 7.6 MgC·ha^{-1} versus 149 ± 6.0 MgC·ha^{-1}, respectively), but stocks of CWD were 2.5 times larger at TNF (16.2 ± 1.5 MgC·ha^{-1} at BDFFP, versus 40.1 ± 3.9 MgC·ha^{-1} at TNF). A model of current forest dynamics suggests that the BDFFP was close to carbon balance, and its size class structure approximated a steady state. The TNF, by contrast, showed rapid carbon accrual to live biomass (3.24 ± 0.22 MgC·ha^{-1}·a^{-1} in TNF, 2.59 ± 0.16 MgC·ha^{-1}·a^{-1} in BDFFP), which was more than offset by losses from large stocks of CWD, as well as ongoing shifts of biomass among size classes. This pattern in the TNF suggests recovery from a significant disturbance. The net loss of carbon from the TNF will likely last 10–15 years after the initial disturbance (controlled by the rate of decay of coarse woody debris), followed by uptake of carbon as the forest size class structure and composition continue to shift. The frequency and longevity of forests showing such disequilibruim dynamics within the larger matrix of the Amazon remains an essential question to understanding Amazonian carbon balance.

Citation: Pyle, E. H., et al. (2008), Dynamics of carbon, biomass, and structure in two Amazonian forests, *J. Geophys. Res.*, *113*, G00B08, doi:10.1029/2007JG000592.

1. Introduction

[2] Tropical forests are an integral part of the global carbon cycle [*Prentice et al.*, 2001], accounting for 32% of global terrestrial NPP [*Field et al.*, 1998]. Changes in tropical forest carbon cycling could alter the pace of climate change [*Adams and Piovesan*, 2005; *Clark*, 2004a; *Clark et al.*, 2003; *Bosquet et al.*, 2000]. Amazonian forests account for about half of the world's undisturbed tropical forest areas [*FAO*, 1993], making quantification of Amazonian carbon stocks, fluxes and dynamics essential to understanding the global carbon cycle.

[3] In the last decade, many studies have attempted to quantify biomass and characterize carbon dynamics of tropical rain forests, yet much uncertainty remains [*Ometto et al.*, 2005]. Site-specific studies of carbon exchange vary in showing Amazonian forests as a net sink for atmospheric carbon [*Malhi et al.*, 1998; *Araújo et al.*, 2002; *Carswell et al.*, 2002], or a source [*Rice et al.*, 2004; *Miller et al.*, 2004; *Saleska et al.*, 2003], but whether these observed patterns are a temporary response to recent disturbance or part of a long-term trend remains uncertain. Field-based estimates of Amazon biomass also vary [*de Castilho et al.*, 2006; *Houghton*, 2005; *Laurance et al.*, 1999; *Malhi et al.*, 2006; *Saatchi et al.*, 2007], with much uncertainty resulting from the spatial variability of forests across the Amazon basin. Studies of plots distributed across the Amazon basin have shown spatial trends in wood density [*Baker et al.*, 2004], productivity [*Malhi et al.*, 2004] and biomass [*Malhi et al.*, 2006] at the near continental scale of the Amazon Basin. Even at the smaller spatial scale of central to eastern Amazon, *Vieira et al.* [2004] showed significant variation in

[1]Department of Earth and Planetary Sciences, Harvard University, Cambridge, Massachusetts, USA.
[2]Biological Dynamics of Forest Fragments Project, National Institute for Amazonian Research, Manaus, Brazil.
[3]Now at Urban Design and Planning, University of Washington, Seattle, Washington, USA.
[4]Universidade de Sao Paulo, Piracicaba, Brazil.
[5]Department of Ecology and Evolutionary Biology, University of Arizona, Tuscon, Arizona, USA.
[6]Smithsonian Tropical Research Institute, Balboa, Panama.

0148-0227/08/2007JG000592$09.00

the size structure of the population of live trees and associated biomass.

[4] Most studies of spatial variation in carbon in Amazonian forests have been limited to live biomass [e.g., *Malhi et al.*, 2006; *Vieira et al.*, 2004; *Baker et al.*, 2004]. Dead organic material is an essential component of the carbon budget and can drive the net carbon balance of an ecosystem [*Barford et al.*, 2001; *Rice et al.*, 2004]. Coarse woody debris (CWD) can comprise as much as 42% of the aboveground biomass in some tropical forests [*Clark et al.*, 2002], constituting a significant biomass pool and contributing a large fraction of the respiratory efflux of CO_2. With the short mean residence time of CWD (~6–8 years) in tropical forests [*Chambers et al.*, 2001a], variations in CWD distributions can shift the balance of carbon in forests and play a major role in ecosystem carbon dynamics [*Rice et al.*, 2004; *Saleska et al.*, 2003].

[5] In this study, we examine forest biomass and dynamics at varying spatial scales. We compare two extensively studied sites in the Amazon, separated by more than 500 km. We characterize the landscape scale (10–100 km^2) variability by examining plots distributed across the landscape at each site. At one of the sites, the measurements appear to have captured the response of the ecosystem to a major mortality event, providing a unique opportunity to observe the legacies of disturbance and the dynamics of recovery.

2. Site Descriptions

2.1. Tapajós National Forest

[6] The Tapajós National Forest (TNF) plots are located near the Santarém-Cuiaba Highway (BR-163), ~80 km south of Santarém (54°58′W, 2°51′S, Figure 1a). The TNF is a 450,000 ha area of closed-canopy upland forest with mean temperature and relative humidity of 25°C and 85 percent respectively. The forest receives an average of 1909 mm of annual rainfall, with a 5 month dry season between July and November, where the dry season is defined as the number of months with mean rainfall <100 mm $month^{-1}$ [*Parotta et al.*, 1995; *Vieira et al.*, 2004]. The soils are nutrient-poor clay oxisols, with little organic matter and low cation exchange [*Silver et al.*, 2000]. Plots are located in primary forest areas, with common emergent species, *Manilkara huberi* (Ducke) Chev., *Hymanaea courbaril* L., and *Tachigalia* sp., considered typical for the region [*Parotta et al.*, 1995]. *Vieira et al.* [2004] reported 133 species ha^{-1} for the TNF. Eddy-flux measurements have been made at km 67 in the TNF [*Hutyra et al.*, 2007; *Saleska et al.*, 2003]. The topography is relatively flat.

2.2. Biological Dynamics of Forest Fragments

[7] The Biological Dynamics of Forest Fragments (BDFFP) plots are located in terra firme (not seasonally inundated) forest in a partially fragmented landscape, 80 km north of Manaus (2°30′S, 60°W, Figure 1b). Rainfall ranges from 1900 to 3500 mm annually, with a mean of 2285 mm^{-1} and a 3-month dry season from July to September [*Vieira et al.*, 2004]. Soils are xanthic ferrasols, nutrient poor soils typical of much of the Amazon basin. Species richness of trees is very high and can exceed 280 species (≥10 cm DBH) per hectare [*de Oliveria and Mori*, 1999], with *Dinizia excelsa* Ducke, *Caryocar villosum* (Aubl.) Pers., and *Duckeodendron cestroides* Kuhl. as common species. In the nearby Cuieras Reserve, eddy-flux measurements have been made since the late 1990s, with results reported by *Malhi et al.* [1998], and *Araújo et al.* [2002]. Although there is little large-scale relief in the area, the terrain is dissected by ridges and valleys with a vertical scale of 30–100 m, in notable contrast to the TNF.

3. Methods

3.1. TNF: Field Measurements

[8] In the Tapajos National Forest (TNF), near the km 67 road marker along the Santarem-Cuiabá Highway, four transects totaling 19.75 ha were established in 1999 in the foot print of the eddy flux tower; these are collectively referred to as the "km 67 site". In 2003, three additional transects (40 m by 2500 m, ~10 ha each) were established in the TNF, departing from the access trails at km 72 and km 117 along the Santarem-Cuiabá highway, for a total of 30 additional hectares. These transects are denoted the "large scale transects", as they are intended to sample the landscape-scale variability of the terra firme forest in the TNF. At all locations, the long and narrow shape of the transects was intended to capture the fine-scale spatial variations inherent to tropical forests, by encompassing treefall gaps and other sources of fine-scale variability (Figure 1). At km 67, transects were laid out in multiple directions to encompass directional variability. Likewise, the long axis of the large scale transects at km 117 ran in a randomly chosen direction, and changed direction within each transect. The long axis of the large scale transect at km 72 ran roughly north to south, perpendicular to the predominant wind direction, as measured by the eddy-flux tower.

[9] For all TNF transects, all trees with diameter at breast height (DBH) greater than 35cm were measured using a DBH tape, tagged, and mapped in an X-Y coordinate system. Tree DBH was measured at 1.3 m unless a buttress or other bole irregularity was present, in which case the DBH was measured just above the buttress [*Clark et al.*, 2001a, 2001b]. Measured trees were identified botanically to species or genus (where species was uncertain); specimens were collected and deposited in the herbarium of the Museo Gueldi, Belém. Small trees with DBH greater than 10 cm were subsampled at all transects. At the km 67 site, small trees were measured in 10 × 1000 m subtransects (3.99 ha total sample area); subtransects extended along the centerline (x axis) of the larger transect from +5 m to -5 m along the shorter y axis (Figure 1a). In the large scale transects, trees ≥10 cm DBH were measured in 3 subplots (10 m × 500 m each, total sample area of 1.5 ha per transect); subplots were located 0 to 500 m, 1000 to 1500 m and 2000 to 2500 m along the longer, "x" axis, and between +5 and +15 m on the y axis, offset from the central transect axis (Figure 1a). At the km 67 site, live trees were measured in July of 1999, 2001 and 2005, with stems identified botanically to species in 1999. These 6 years of measurements provide a clear record of live tree dynamics. In the large scale transects, live trees were measured in July of 2003 and 2005, providing spatial context for longer term dynamics measured at km 67.

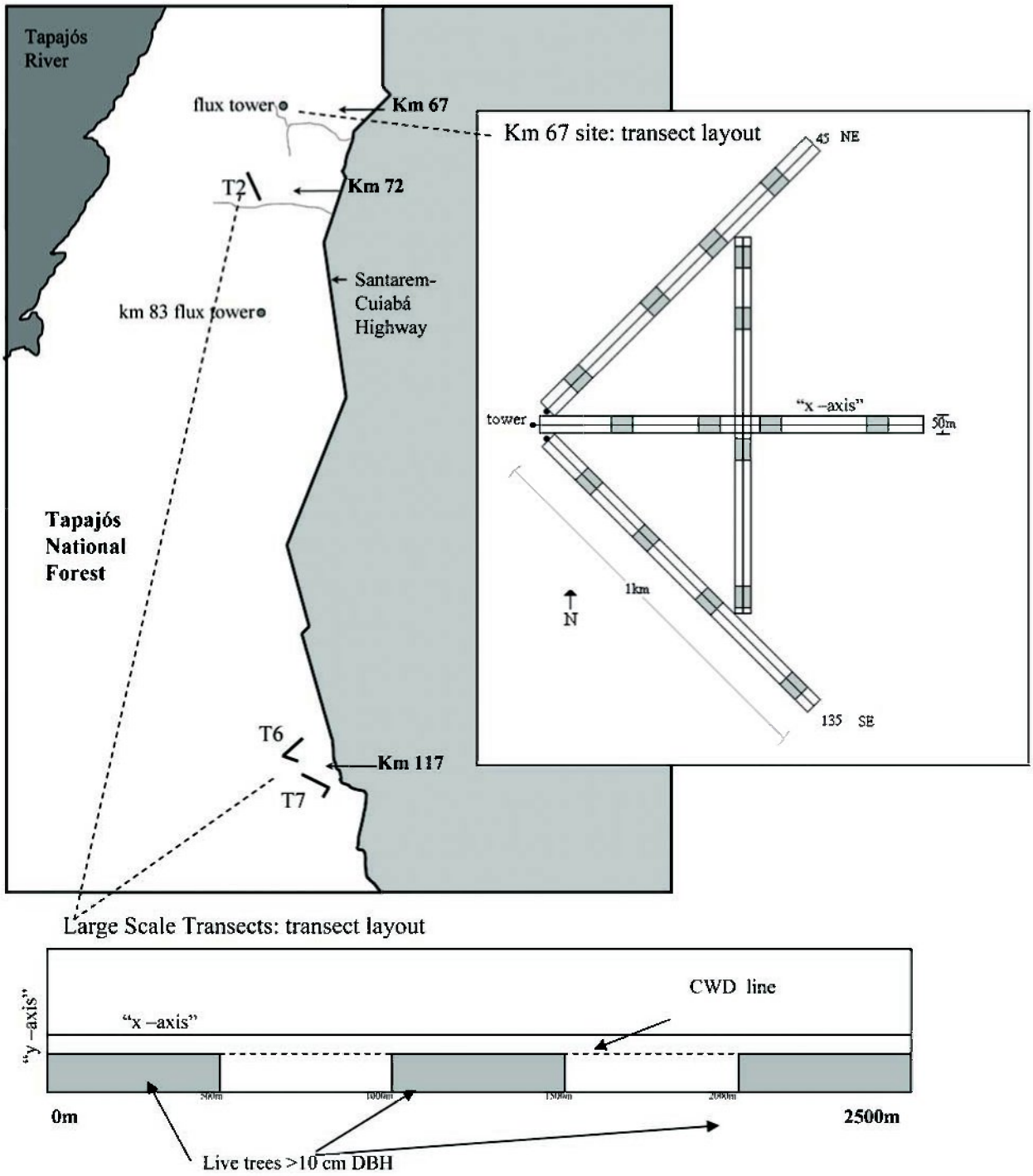

Figure 1a. Locations of research plots in the Tapajós National Forest, Pará, Brazil (TNF, 54°58′ W, 2°51′S), with diagrams of transect designs. In the four transects (50 m × 1000 m) at the km 67 flux tower site, live trees > 35 cm DBH measured in whole transect, trees > 10 cm, <35 cm DBH subsampled along transect centerline, and CWD measured in plots shown by shading. In the "large scale" transects (40 m × 2500 m) at km 73 and km 117, live trees > 35 cm DBH measured in whole transects, with shaded portions showing location of small tree (>10 cm, <35 cm DBH) subsampling, and line for CWD measurements noted.

[10] Coarse woody debris (CWD) was divided into two categories: standing CWD (snags) and fallen CWD. Standing CWD, defined as dead trees standing or at ≥45° angle, with height greater than 1.3 m, and diameter > 10 cm, were measured in the live tree plots for all transects. For standing CWD, DBH was measured and height estimated visually by experienced local forestry technicians, except in the rare

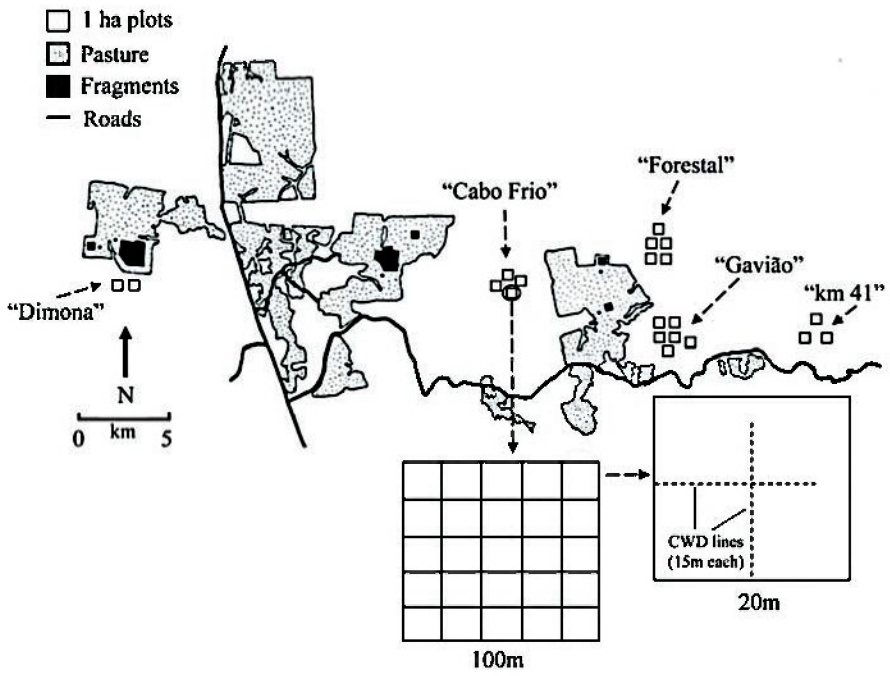

Figure 1b. Locations of 1 ha plots (100 m × 100 m) in BDFFP (2°30′ S, 60° W) used in this study. All plots were located well within the intact forest areas, not forest fragments. Groupings of plots in close proximity are considered "subsites" for analysis. Live trees > 10 cm DBH were measured in each 1 ha plot. CWD was measured using crossing 15 m lines in each 20 m by 20 m subplot. Plot symbols not to scale.

cases where height was less than ~2 m and could be measured with a tape.

[11] At the km 67 site, fallen CWD stems (<45° angle, > 10 cm diameter and > 1 m length) were measured using fixed area plots randomly distributed within the live tree transects (Figure 1a, and described in detail by *Rice et al.* [2004]). Two size classes of dead wood were measured in nested subplots (10–30 cm, and greater than 30 cm). Top, middle and bottom diameters and total length were measured for fallen CWD with either a large tree caliper or a small electronic caliper. *Rice et al.* [2004] demonstrated the compatibility of line intercept and plot based CWD estimates by sampling CWD using both methods at the km 67 site; they found that the two methods agreed within sampling uncertainty. For the large scale transects in this study, fallen CWD was sampled using the line-intercept method [*Van Wagner*, 1968; *Brown*, 1974], also known as planar intercept sampling. The sampling line (~2500 m in total length per transect) was set parallel to the long axis of the transect, but offset 5 m from the foot paths (Figure 1a). The sampling line was then divided into 10 m segments in which the diameter of CWD (≥7.5 cm) that crossed the sampling line was measured.

[12] All CWD measured in the TNF was classified by decay classes 1 through 5 [cf. *Harmon and Sexton*, 1996]. Decay classes were defined as follows: decay class 1, solid wood, recently fallen, bark and twigs present; decay class 2, solid wood, significant weathering, branches present; decay class 3, wood may be sloughing but nail still must be pounded into tree; decay class 4, wood sloughing and/or friable, nails may be forcibly pushed into log; and decay class 5, wood friable, barely holding shape, nails may be easily pushed into log.

3.2. BDFFP: Field Measurements

[13] In the BDFFP plots, live biomass was sampled in 20 individual 1 ha plots (100 m by 100 m) distributed through a 100,000 ha area (Figure 1b). Plots were selected using stratified random sampling and located well within continuous forest, not fragmented areas considered in the larger BDFFP experiment [cf. *Lovejoy et al.*, 1986; *Laurance et al.*, 2002]. Groupings of plots in close proximity are considered "subsites" for analysis. Between 1997 and 1999, diameters of all trees ≥10 cm DBH were measured at 1.3 m in height or above the tallest buttress;measured trees were tagged, mapped and identified botanically to species. Botanical specimens were collected and deposited in the BDFFP herbarium. Plots were recensused between 2002 and 2004 when all new trees of ≥10 cm DBH were marked, mapped, and identified. The surviving trees had their DBH measured, and mortality of trees living in the initial census was noted. Plots were recensused in roughly the order of initial census to keep census interval consistent, such that for individual plots, the census interval ranged from 4.3 years to a maximum of 5.4 years, with a mean interval of 4.7 years. Standing dead trees (CWD) were surveyed with live trees: DBH was measured and height estimated visually by experienced local forestry technicians, except in the cases where height was less than 8 m and could be measured with an aluminum measuring pole. For each plot, fallen CWD (≥10 cm diameter) was measured using the line-intercept method [*Van Wagner*, 1968; *Brown*,

1974], in either 1999 or 2000 in 13 subplots (20 m by 20 m) per plot. Each 1 ha plot was divided into 25 subplots (400 m^2 * 25 subplots = 1 ha) and every second subplot was sampled (in a checker-board pattern) to ensure nearly uniform coverage of the plot. Within each subplot, two 15 m long perpendicular transects were established (yielding 26 transects per plot) in North-South and East-Western cardinal directions (Figure 1b). The decay of CWD was classified as "sound" or "rotten" as defined by *Delaney et al.* [1998].

3.3. Scaling Biomass and Estimating Carbon Fluxes

[14] For all sites, live biomass of each tree was estimated using the allometric equation in *Chambers et al.* [2001a]:

$$\text{Biomass} = \exp\left(-0.37 + 0.333*\ln(\text{DBH}) + 0.933*[\ln(\text{DBH})]^2 - 0.122*[\ln(\text{DBH})]^3\right) \quad (1)$$

[15] This equation was selected to estimate total biomass per tree, since species identification, height and wood density values were not available for all areas surveyed, and the scope of this study was limited to the central and eastern Amazon, where the equation was derived.

[16] To look at the effect of wood density on live biomass estimation, we did an analysis of the subset of plots, km 67 in the TNF and the BDFFP plots, where trees were identified botanically to species. We used the moist forest equation in *Chave et al.* [2005], which includes wood density:

$$\text{Biomass} = \text{density}*\exp(-1.499 + 2.1481*\ln(\text{DBH}) + 0.207*[\ln(\text{DBH})]^2 - 0.0281*[\ln(\text{DBH})]^3) \quad (2)$$

[17] Wood densities were taken from the compiled list in *Chave et al.* [2006]. When available, species-specific densities were used; otherwise trees were assigned mean genus density (identified trees), or site mean density (unidentified trees).

[18] Tree growth, or biomass increment, was determined as the difference between paired biomass measurements for all trees present and alive in both initial and final surveys for the time increment. Growth rates were screened by examining trees for which the data fell outside the central 99% of the frequency distribution of growth rates (> -3.5 cm • a^{-1}, < 5.3 cm • a^{-1}). Closer inspection showed individual trees with growth rates as high as 6.7 cm • a^{-1} measured consistently and correctly over the 6 year interval of the TNF km 67 study, so the maximum growth rate was set to 6.7 cm • a^{-1}, with -3.5 cm • a^{-1} remaining as the minimum growth rate. Mortality was the summed biomass of all trees that died in the time interval. Recruitment was the summed biomass of all trees that attained minimum size of 10 cm DBH during the study period.

[19] Sampling uncertainties around these biomass quantities were calculated by bootstrap analyses [*Efron and Tibshirani*, 1993]. Bootstrap samples of 1 ha subplots were drawn 1000 times with replacement to estimate 95% confidence intervals around carbon stocks, growth, recruitment, mortality, and tree density. We used 1ha subplots as the unit of replication because they are larger than canopy gaps and thus avoid underestimating sample variance due to psuedoreplication [*Hurlbert*, 1984]. Asymmetrical confidence intervals are reported symmetrically where reported confidence limits are the maximum of (97.5 percentile – median) and (median – 2.5 percentile) (as in the work of *Rice et al.* [2004]).

[20] For the plot-based CWD measurements at km 67, dimensional measurements were scaled to volumes by using the following taper function from *Chambers et al.* [2000] to calculate a top diameter from a DBH and an estimated height.

$$\text{Top Diameter} = 1.59*\text{DBH(cm)}*(\text{Height(m)}*100(\text{cm/m}))^{-.091} \quad (3)$$

[21] The calculated top diameter and DBH were averaged to obtain a middle diameter and these three values were converted to disk areas and entered into Newton's formula to calculate a volume. For the line intercept measurements in both TNF and BDFFP, CWD volumes were estimated using the formula from *Van Wagner* [1968].

$$\text{wood volume} = (\pi^2 \cdot \Sigma\text{diameter}^2)/(8 \cdot \text{line length}). \quad (4)$$

[22] For the line-intercept measurements at the TNF site, volumes were converted to biomass with site-specific, decay class specific CWD densities described above [*Palace et al.*, 2007; *Rice et al.*, 2004]. For the line-intercept measurements at the BDFFP sites, volumes were converted to necromass using average Amazon tree wood density from *Fearnside* [1997] for CWD in the "sound" class, and site-specific decayed wood density from *Cummings et al.* [2002] for CWD in the "rotten" decay class.

[23] For the 1999–2001 time interval at km 67, the large scale transects, and the BDFFP plots, losses of carbon to the atmosphere from CWD decomposition were estimated assuming that respiration followed first-order kinetics, where respiration = k × total CWD, and k was a decay-class-specific respiration rate [see *Rice et al.*, 2004; *Chambers et al.*, 2001b]. For the second time step (2001 – 2005), 2005 CWD pool size and 2001–2005 respiration rate were estimated based on a simple model of monthly respiration rates, where the total CWD at time 2 was equal to the preceding month's CWD plus additions due to mortality, less estimated respiration. (described by *Hutyra et al.* [2008]). Sampling errors on downed CWD and respiration were also calculated by bootstrap, with individual plots serving as the unit of replication for the plot-based measurements at km 67, and individual line segments serving as the unit of replication for line intercept measurements at other TNF transects. Errors for standing CWD were bootstrapped where subplots were the unit of replication, much like live trees. Errors for total CWD were constructed by combining bootstraps. For all quantities, dry weight of woody biomass was converted to mass in carbon using the relationship that 50% of dry biomass is attributed to carbon [*Brown*, 1997].

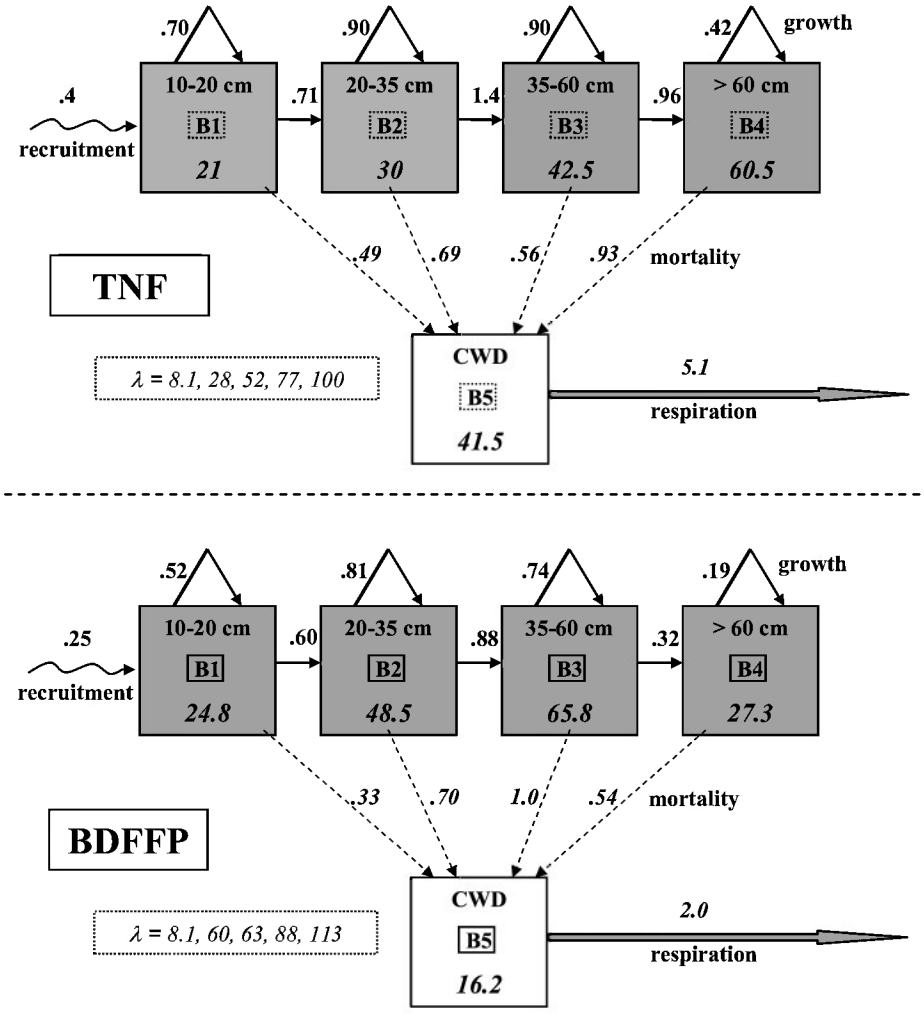

Figure 2. Schematic diagram of organic stocks (Mg C/ha, in large boxes) and fluxes (growth: solid straight arrows, mortality: dashed arrows, recruitment: wavy arrow) (Mg C/ha/a) at the (top) TNF and (bottom) BDFFP during the study period. B1–B4 represent size classes of live trees; B5 represents CWD. The time constants for the eigenmodes of the associated linearized model (λ) are given in years. BDFFP stocks are all close to balance with only small amounts of CO_2 being taken up by the smallest trees or stored as CWD. In contrast, TNF shows vigorous accumulation of biomass in B2 and B3, and strong net loss of CWD.

3.4. Site Comparisons

[24] To assess consistency of fluxes in the LT transects over the 2 year period with the longer term fluxes at km 67, we compared the mean live biomass fluxes of the km 67 site over the 6 year period of measurement with the mean fluxes in the large scale transects, and found they were not significantly different for growth and mortality (growth increment: $t = -0.3185$, $df = 46$, p-value = 0.7515; mortality: $t = 1.2548$, $df = 46$, p-value = 0.2159) and marginally significant for recruitment (recruitment: $t = 2.1933$, $df = 47$, p-value = 0.0333). Given this compatibility, we used both the km 67 measurements (from 2001 to 2005) and the shorter term LT transects (from 2003 to 2005) to calculate TNF site means.

[25] For comparison between the TNF and BDFFP sites, a p-value to indicate significant site differences was generated by taking the difference between the bootstrapped samples: the probability of the two sites being the same, thus depends on the number of times the bootstrapped differences deviate from the expected difference, in this case, either TNF site mean > BDFFP site mean, or TNF site mean < BDFFP site mean. In cases where data were divided into individual subplots, significance of site differences was also determined by using standard statistical tests for the difference between means, either t test or Wilcoxon rank-sum, where individual 1 ha subplots served as replicates. (Generation of the 1 ha subplots is described in more detail in the section on subsampling and spatial analysis, below.)

3.5. Model of Near-Term Mass Fluxes

[26] In order to characterize site differences in carbon dynamics, we constructed a simple box model of above-ground woody biomass, where each box represents a size class of live biomass and the 5th box represents CWD (Figure 2). Each live class accumulates biomass within the class, transfers biomass into the next larger size class, and dies, at rates which we approximate using 1st-order kinetics

Table 1. Live Biomass and Live Biomass Fluxes as Calculated Using DBH Only (Allometric Equation From *Chambers et al* [2001a]) Compared to Values Calculated Using DBH and Wood Density (Allometric Equation From *Chave et al.* [2005])[a]

	TNF (km 67 Only)		BDFFP	
	DBH and Wood Density	DBH Only	DBH and Wood Density	DBH Only
Total Live Biomass ($MgC \bullet ha^{-1}$)	197 (±11.6)	151 (±5.5)	190 (±9.8)	167 (±7.6)
Live Biomass, <100 cm DBH	158 (±7.6)	133 (±5.6)	181 (±10.1)	162 (±8.6)
Growth ($MgC \bullet ha^{-1} \bullet a^{-1}$)	3.76 (±0.22)	3.16 (±0.23)	3.08 (±0.22)	2.59 (±0.16)
Recruitment ($MgC \bullet ha^{-1} \bullet a^{-1}$)	0.39 (±0.09)	0.45 (±0.10)	0.24 (±0.04)	0.25 (±0.04)
Mortality ($MgC \bullet ha^{-1} \bullet a^{-1}$)	3.61 (±1.02)	2.97 (±0.69)	2.79 (±0.57)	2.56 (±0.48)

[a]Numbers for TNF include only the km 67 subset of plots, where botanical species identification allowed densities to be determined. Standing live biomass appears more sensitive to allometry and wood density than fluxes. Parentheses contain 95% confidence intervals calculated by bootstrap.

(rate proportional to the biomass in the class). The total growth of trees in a given size class is the sum of growth-within-class and growth -into-next-larger class, and thus the latter represents a loss of biomass from the smaller size class. All coefficients were determined from directly measured pool sizes and fluxes, except respiration which was estimated as described above (Figure 2). This simple box model represents an estimate of the tangent-linear approximation to the real ecosystem dynamics, similar to the more sophisticated model described by *Chambers et al.* [2004] for a forest near Manaus. We use this box model to assess short-term tendencies of the biomass distribution at each site.

3.6. Spatial Analysis and Sample Size Requirements

[27] We used a simulated sampling approach to assess spatial variation within the two sites, and to explore minimum size requirements for adequate biomass and carbon dynamics sampling [e.g., *Keller et al.*, 2001; *Chave et al.*, 2003]. We divided transects in the TNF study into nonoverlapping 1 ha subplots along the *y* axis (every 200 m for km 67 transects, every 250 m for large scale transects) and calculated biomass, $stems \bullet ha^{-1}$, increment, recruitment, and mortality for each subplot. For subsampled small trees in the km 67 transects, the narrower transects were divided every 200 m on the *y* axis to yield 0.2 ha subplots, proportional to the 1 ha subplots for large trees. For the subsampled trees in the large scale transects, the three small-tree subplots were assembled as a continuous transect, and then divided every 150 m to yield 10, 0.15 ha non-overlapping subplots, which were matched by distance to the closest 1 ha large tree plot. Thus, the subsampling strategy used in the TNF was incorporated into the simulated subplots, where each 1 ha subplot represents a 1 ha sample for trees > 35 cm DBH and an associated subsample of 0.15 – 0.20 ha of tree > 10 cm and <35 cm DBH. For the BDFFP site, we used the existing 1 ha plots. We chose 1 ha plots because it is a typical plot size for studies characterizing tropical forests [e.g., *Nascimento and Laurance*, 2002; *de Castilho et al.*, 2006; *ter Steege et al.*, 2003]. We used a Monte-Carlo approach to look at requirements for accurate estimation. We drew 1000 random samples of 1 ha plots at a range of total sample sizes (i.e., number of 1 ha plots). For a given parameter (e.g., biomass, growth increment), we estimated an "adequate sample" as the number of plots required to yield a coefficient of variation (confidence interval/mean) < 20%, 95% of the time.

[28] In many previous studies using similar simulated sampling approaches [*Keller et al.*, 2001; *Chave et al.*, 2003; *Clark and Clark*, 2000], samples have all been drawn from contiguous/semi-contiguous plots or plot networks where maximum distances between subplots were 1 to 5 km. Our approach sampled plots separated by much greater distances (up to 50 km), as in *Nascimento and Laurance* [2002]. To look at spatial trends over these distances, we constructed variograms of the 1 ha subplots used in the simulated sampling for biomass, growth increment and mortality, by plotting proximate distance versus squared difference for all possible pairs of 1 ha plots in both the TNF (1128 possible pairs) and the BDFFP (190 possible pairs). Because the recruitment occurred only in the small tree subplots in the TNF, we did not construct a variogram for this quantity.

4. Results

4.1. Carbon in Standing Biomass

[29] The BDFFP site held roughly 12% greater aboveground live biomass than the TNF site, with 167 ± 7.6 $MgC \cdot ha^{-1}$ in the BDFFP and 149 ± 6.0 $MgC \bullet ha^{-1}$ in the TNF (Tables 1 and 2). However, the differences were not significant when biomass was calculated using the *Chave et al.* [2005] allometry, which yielded 197 ± 11.6 $MgC \bullet ha^{-1}$ in

Table 2. Live Biomass and Coarse Woody Debris at Subsites in the Tapajós National Forest and BDFFP Near Manaus[a]

	Live Biomass ($MgC \cdot ha^{-1}$)	Live Stems (ha^{-1})	Fallen CWD ($MgC \cdot ha^{-1}$)	Standing CWD ($MgC \cdot ha^{-1}$)
		Tapajós		
km 67	149 (±5.5)	480 (±49)	35 (±4.8)	8.9 (±1.9)
km 72	156 (±9.6)	428 (±33)	29 (±5.6)	13 (±2.8)
km 117	152 (±17)	460 (±33)	37 (±18)	3.9 (±1.5)
km 117	146 (±15)	435 (±66)	35 (±14)	8.6 (±3.7)
Mean	149 (**±6.0**)*	441 (**±43**)*	32 (**±3.7**)**	8.7 (**±1.3**)**
		BDFFP		
Gavião	150 (±16)	597 (±19)	12 (±2.2)	3.7 (±1.8)
Florestal	177 (±22)	634 (±22)	18 (±3.6)	1.7 (±0.6)
KM 41	172 (±24)	622 (±25)	11 (±2.3)	4.0 (±1.8)
Dimona	181 (±43)	688 (±43)	9.5 (±2.9)	4.9 (±2.8)
Cabo Frio	166 (±51)	608 (±52)	12 (±3.2)	2.8 (±2.1)
Mean	167 (**±7.6**)*	621 (**±39**)*	13 (**±1.3**)**	3.2 (**±0.8**)**

[a]Site means appear in bold. Parentheses contain 95% confidence intervals. * Site means significantly different, Wilcoxon rank sum test $p < 0.01$, for 1 ha subplots. ** Site means significantly different, $p < 0.01$, for bootstrapped differences. CWD, coarse woody debris.

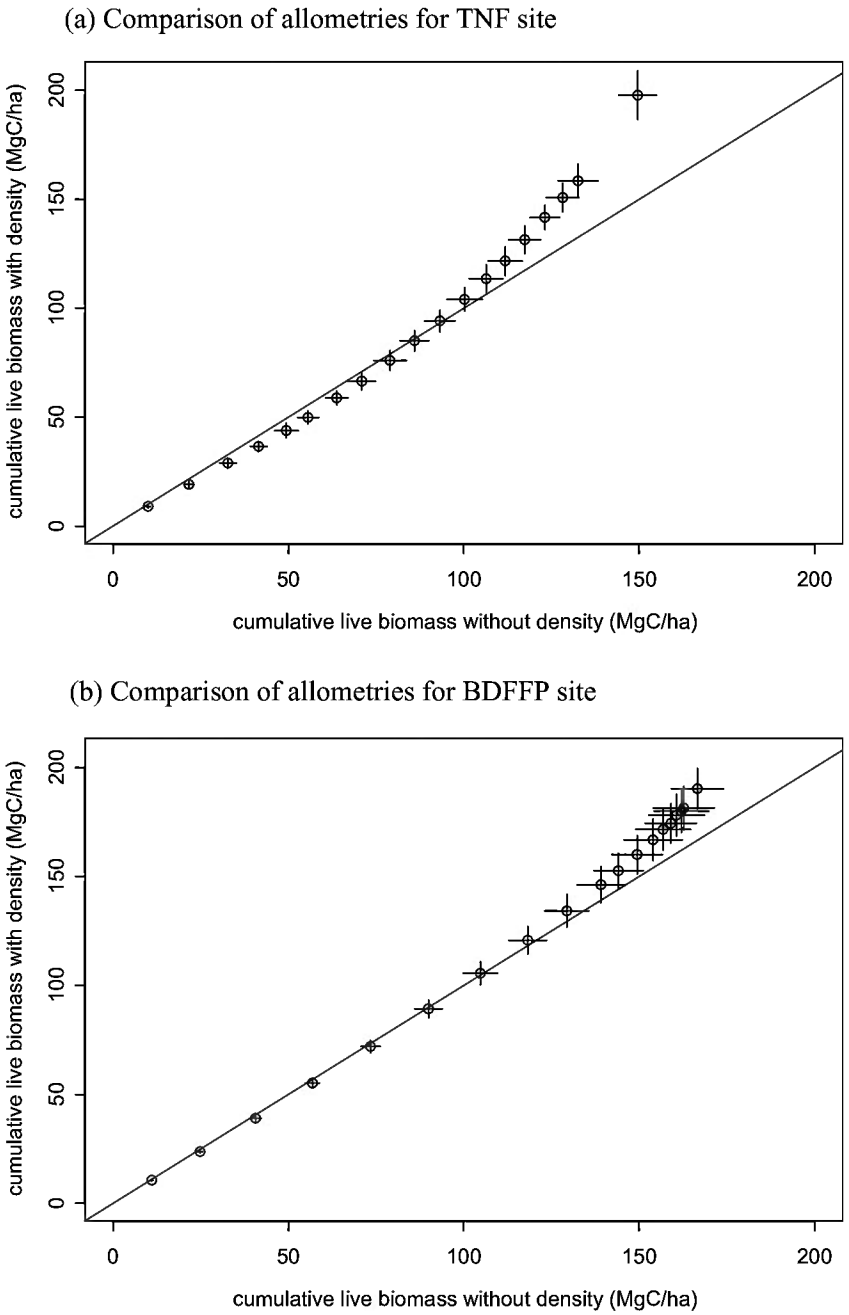

Figure 3. Quantile-quantile plots of cumulative carbon in live biomass by size class calculated using allomtery of *Chambers et al.* [2001a] (without wood density) versus live biomass by size class calculated using allometry of *Chave et al.* [2005] (includes wood density), for (a) TNF and (b) BDFFP. Comparison with one to one line shows allometries yield similar values for live biomass, except in the largest size classes (>100 cm DBH). Error bars show 95% confidence interval calculated by bootstrap.

the TNF and 190 ± 9.8 MgC•ha^{-1} in the BDFFP. Much of this difference was due to the greater weight the *Chave et al.* [2005] allometry gave to the largest size class of trees (Figure 3); the two allometries yielded values that diverged significantly from the 1 to 1 line after size classes > 100cm DBH were included.

[30] Both sites showed low variability of biomass at the landscape scale (Table 2). Within the TNF, carbon in live biomass for individual transects ranged from 146 ± 15 MgC•ha^{-1} to 156 ± 9.6 MgC•ha^{-1} in 2003 (Table 2). For BDFFP plots, individual subsites ranged from 150 ± 16 MgC•ha^{-1} and 181 ± 43 MgC•ha^{-1}; greater variation in BDFFP plots may reflect the smaller total area sampled at each BDFFP subsite (2–6 ha, versus 10–20 ha sampled at each TNF transect). In the TNF transects, analysis of 1 ha subplots within the larger transects yielded more variable live biomass values (112 to 187 MgC•ha^{-1}) than the TNF transects.

[31] Live biomass at the two sites showed structural differences similar to those reported by *Vieira et al.*

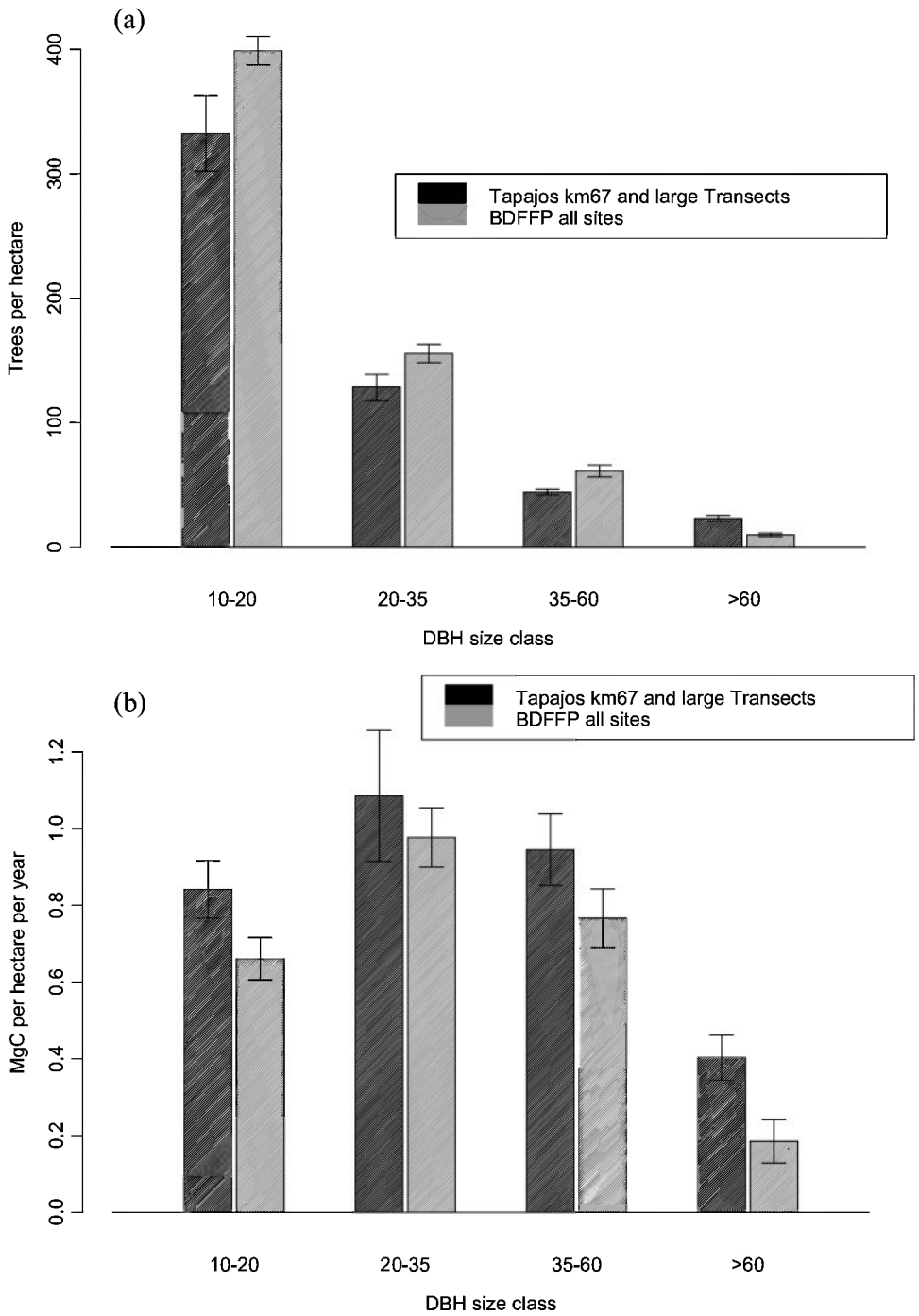

Figure 4. Stems per ha and live tree growth by size class for both the TNF and the BDFFP. Error bars show bootstrapped 95% confidence interval. For all size classes, sites were significantly different ($p < 0.01$) for both stems per ha and growth, except in the 20 to 35 cm DBH size class, where growth increment was statistically indistinguishable. The BDFFP sites show more trees (larger tph) in the smallest size class, but smallest size class at the TNF shows larger uptake of carbon.

[2004]. The BDFFP site had significantly higher stem counts, with a mean of over 621 ± 39 stems•ha^{-1}, versus a mean value of 441 ± 43 stems•ha^{-1} at the TNF (Table 2 and Figure 4a, unpaired t-test of 1 ha plots: $t = -10.1116$, $df = 67$ p-value = 0). These stems were distributed among size classes differently: The BDFFP plots showed significantly higher stem counts in the small and middle size classes, while the TNF showed significantly more stems in the largest size class (Figure 4a, $p < 0.01$ for unpaired t.tests by size class). Biomass in live trees was also distributed differently at the two sites (Figure 5a, Two Sample Kolmogorov-Smirnov Test: $ks = 0.474$, $p = 0.0267$), with more live biomass concentrated in the smallest and largest size classes in the TNF, relative to the BDFFP plots which

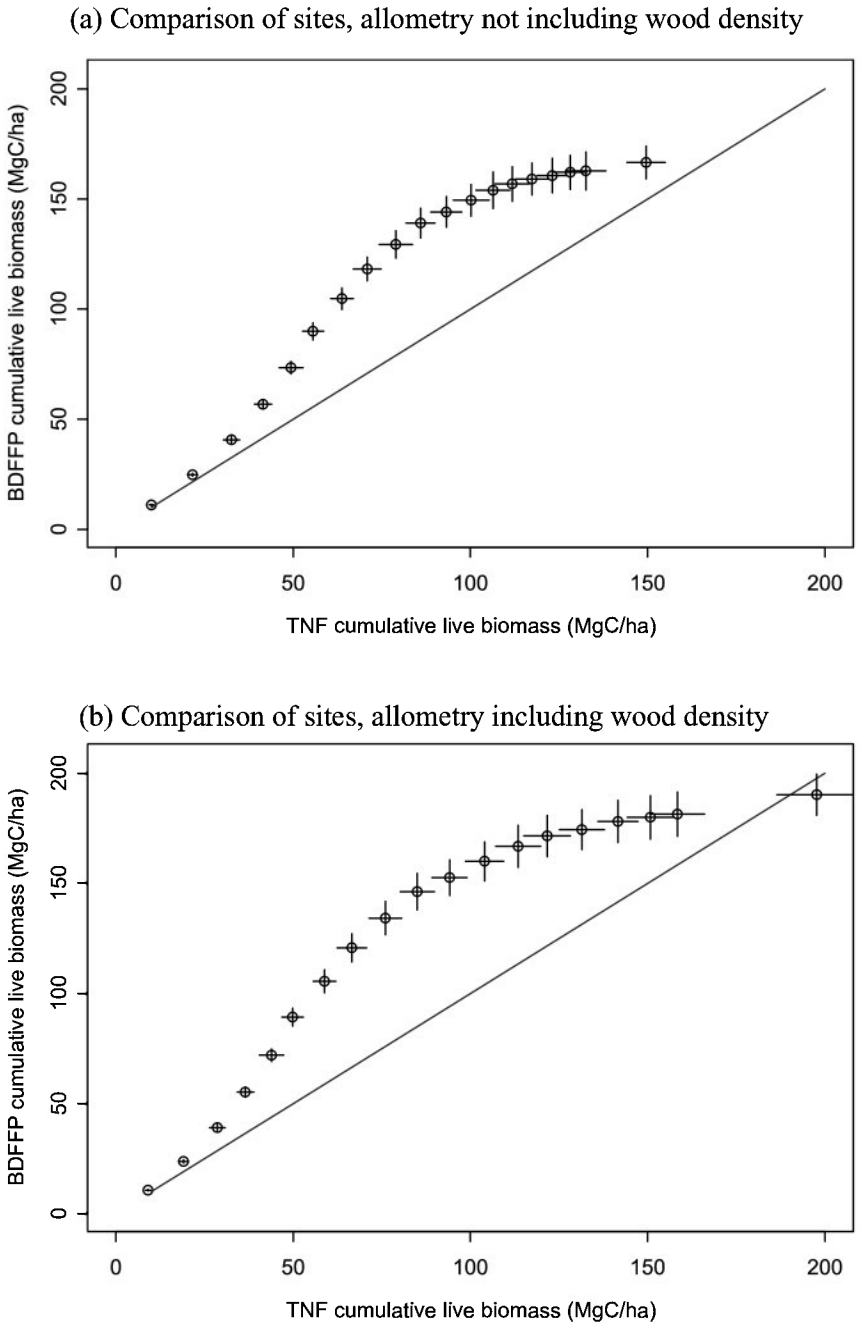

Figure 5. Quantile-quantile plots of cumulative carbon in live biomass by size class for TNF versus BDFFP, using (a) all plots for each site, allometry of *Chambers et al.* [2001a] (without wood density) and (b) km 67 subset of TNF plots and BDFFP plots, using allometry of *Chave et al.* [2005] which includes wood density. One to one line shown. Curved portion in middle results from higher biomass in middle size classes at the BDFFP site. Figures 5a and 5b show the same form, despite differences in allometry, indicating that observed site structural differences are not sensitive to wood density effects. Error bars show 95% confidence interval calculated by bootstrap.

had greater biomass in the middle size classes. Notably, these structural differences were consistent, even when wood density was incorporated in the allometry (Figure 5b), indicating that observed structural differences were not confounded with wood density effects.

[32] Site differences were even more pronounced for CWD: TNF transects contained a mean of 40.1 ± 3.9 MgC•ha^{-1}, 2.5 times as much as the BDFFP with16.2 ± 1.5 MgC•ha^{-1} (for bootstrapped differences, $p < 0.001$; also see Table 2). These regional site differences were far greater than the within site, landscape scale variation. CWD values for TNF transects ranged from 41 to 44 MgC•ha^{-1}, while CWD values for BDFFP plots ranged from 14 to 20 MgC•ha^{-1} (Table 1). At both sites, the proportion of CWD biomass in standing dead trees varied from 10 to 30%, with a mean of about 20%. Overall, the TNF showed a significantly larger

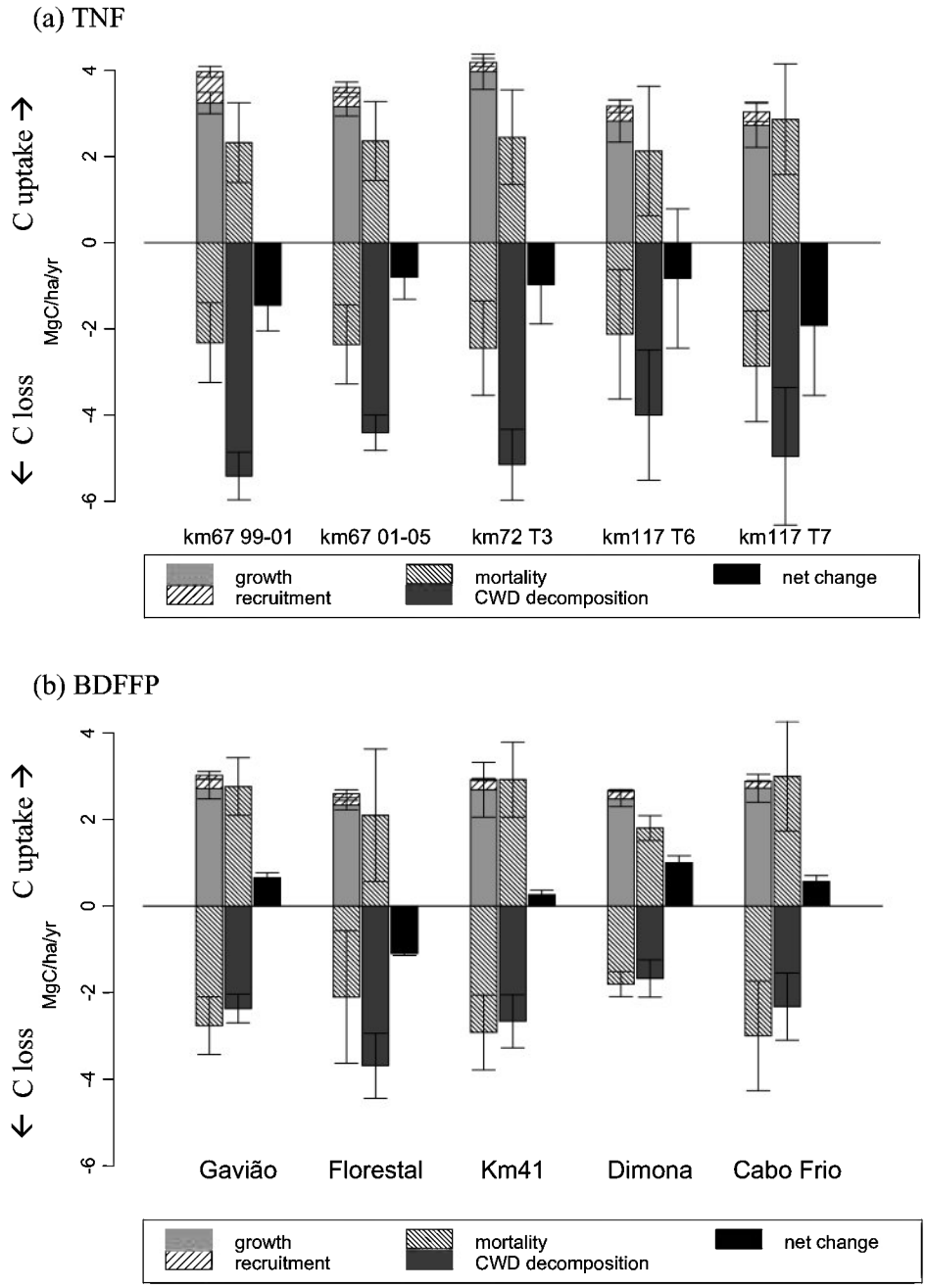

Figure 6. Carbon fluxes in live and dead biomass at nine sites in the (a) TNF and (b) BDFFP. For each site, bars on left represent fluxes in live biomass. Bars in the middle represent fluxes in dead biomass, and black bars on right show combined net flux in live and dead biomass. Error bars show 95% confidence interval derived from bootstrap analysis. Most TNF sites show net loss for carbon to the atmosphere, while BDFFP sites appear to be net neutral or storing carbon.

CWD pool, both standing and fallen, across all of the transects.

4.2. Carbon Fluxes in Live and Dead Biomass

[33] The gross fluxes in both live and dead biomass at TNF (Figure 6a) were larger than those at the BDFFP sites (Figure 6b), despite the lower stem counts (Table 2), and regardless of which allometry was applied (Table 1). At the TNF, greater growth in individual trees, particularly in the smallest size classes (Figure 4b), resulted in an overall ~20% greater rate of carbon accumulation through growth. The larger pool of CWD measured in the TNF (Table 1) resulted in larger estimated fluxes of carbon from decomposition in all areas of the TNF (Figure 6a), relative to the BDFFP plots (Figure 6b).

[34] In the TNF, the live biomass pool accrued carbon, with growth and recruitment exceeding mortality losses for most transects and time intervals (Figure 6a). For individual transects, the net live biomass flux ranged from uptake of 0.6 to 2.0 $MgC \bullet ha^{-1} \bullet a^{-1}$, with an average uptake of

Table 3. Site Mean Carbon Fluxes[a]

	TNF	BDFFP
Growth	3.24 (±0.22)	2.59 (±0.16)*
Recruitment	0.36 (±0.074)	0.25 (±0.041)
Mortality	2.59 (±0.52)	2.56 (±0.48)
CWD Respiration	4.70 (±0.39)	2.66 (±0.33)**
Net Flux	−1.02 (±0.45)	0.18 (±0.31)**
NEE Eddy-Flux Tower	−0.89 (±0.22)[b]	1 to 8[c]

[a]Units are in MgC•ha^{-1}•a^{-1}. TNF shows larger gross fluxes, and likely net loss. BDFFP site shows smaller gross fluxes and likely carbon balance in live and dead biomass. Parentheses contain 95% confidence intervals calculated by bootstrap. * Site means significantly different, Wilcoxon rank sum test, $p < 0.001$. ** Site means significantly different, $p < 0.001$, for bootstrapped differences.
[b]*Hutyra et al.* [2007].
[c]*Araújo et al.* [2002].

0.8 MgC•ha^{-1}•a^{-1}. However, estimated respiration flux from the large CWD pool exceeded the measured mortality inputs for most subsites (Figure 6a), leading to net loss of carbon from CWD, to the atmosphere ranging from −0.81 ± 0.51 to −1.9 ± 1.6 MgC•ha^{-1}•a^{-1}. At two subsites, uncertainty around the net flux suggested potential neutral carbon emission, but for the majority of subsites, the result was an overall carbon loss from the forest to the atmosphere in the TNF despite significant increases in live biomass; this result is consistent with eddy flux measurements [*Saleska et al.*, 2003; *Hutyra et al.*, 2007].

[35] Our modeled CWD respiration is supported by a partial resurvey of CWD at the TNF km 67 site in 2006, which showed a decline of 23% between 2001 and 2006. Our modeled results predicted a 21% decline in CWD stocks. Our model may slightly underestimate CWD losses, since the model only accounted for C lost through respiration, and not fragmentation of CWD pieces.

[36] The BDFFP sites also showed accrual in live biomass (Figure 6b), with an average increase of 0.27 MgC•ha^{-1}•a^{-1}. The estimated net flux from the CWD pool varied from a small source (−1.6 MgC·ha^{-1}) to a small sink (0.35 MgC•ha^{-1}•a^{-1}) in different plots. As a result, estimates of overall net flux in the BDFFP sites (summing fluxes in live and dead biomass) range from slightly positive to neutral (Figure 6b), with mean uptake of 0.18 ± 0.29 MgC•ha^{-1}•a^{-1}, statistically indistinguishable from zero.

[37] Overall rates of mortality in terms of carbon in the TNF and BDFFP were not significantly different, with 2.59 ± 0.52 MgC·ha^{-1} in the TNF and 2.56 ± 0.48MgC·ha^{-1} at the BDFFP site (Table 3, Wilcoxon rank-sum: W = 1641, n = 48, m = 20, p-value = 0.8465). Because the stem counts were higher in the BDFFP, the equivalent mortality in terms of carbon corresponded to annualized stem mortality rates of 1.9% per year for TNF and 1.6% per year for BDFFP. Examination of mortality rates by size class suggested higher mortality rates at the TNF in the smallest size class, 10 – 20 cm DBH (Figure 7a), though subsampling analysis showed mortality was not well sampled at our sites, particularly for the TNF (see below). As a proportion of live stems (Figure 7b), mortality was more evenly distributed across size classes at the BDFFP plots, with a possible increase in percentage mortality for the largest size class. For the TNF, percentage mortality was again concentrated in the smallest size classes, with 2.2 ± 0.20% mortality in the 10–20 cm size class at the TNF compared to 1.4 ± 0.16% in the same size class at BDFFP (Figure 7b). The 20 to 35 cm size class at the TNF showed 2.0 ± 0.47% mortality, a value not significantly different from the 1.4 ± 0.33% mortality measured in the same size class at the BDFFP.

4.3. Sample Size Requirements and Spatial Analysis

[38] Simulated sampling showed biomass, trees•ha^{-1}, and growth increment were all well sampled for both sites, with all these quantities reaching coefficient of variations (our measure of "adequacy" of estimate) of well below 20% (Figure 8). For stem density (not included in the figure), coefficient of variation reached ∼5% for the full area sampled in the TNF, and ∼4% for all 20 ha sampled in the BDFFP. For mortality and recruitment, however, both sites fell short of the minimum ratio, with the coefficient of variation for mortality reaching 21% in the BDFFP and 24% in the TNF and the coefficient of variation for recruitment reaching only 22% in the BDFFP and 26% in the TNF.

[39] Where there is spatial variability at the landscape scale, a variogram of similarity would be expected to show a trend of decreasing similarity with increasing distance between plots, however, our spatial analyses (variogram) for both TNF and BDFFP plots showed no pattern in similarity with distance. Pair wise plot differences showed the same range of values at all distances, suggesting no spatial correlation for biomass, growth, and mortality within the plots at the two sites.

5. Discussion

5.1. Site Differences in Dynamics and Structure

[40] The gross fluxes of growth and CWD respiration were larger in the TNF than the BDFFP plots, indicating higher rates of turnover and a more dynamic forest in the Tapajós. More carbon was taken up through growth of live trees in the TNF, particularly in the smallest size classes (Figure 4), despite the slightly lower overall stem counts (Table 2). *Malhi et al.* [2006] and *Baker et al.* [2007] suggested that on a continental scale, forests in the western Amazon are more dynamic than central and eastern Amazon forests, where mean wood density is inversely correlated with forest dynamics [*Malhi et al.*, 2004]. We compare sites on a smaller scale (within the central to eastern Amazon) and with very similar mean wood density (0.66 g•cm^{-3} for TNF and 0.69 g•cm^{-3} for BDFFP). The site differences in dynamism we found on this smaller scale may still fit in with the continental trends described by *Malhi et al.* [2006], particularly where some of the dynamism observed in the TNF may reflect past disturbance.

[41] The sites also showed stand structural differences in the distribution of live trees consistent with the observed differences in growth and stand dynamics. The BDFFP site had higher stem densities and greater biomass in small and middle size classes. We have observed that small trees in the TNF accumulated carbon more rapidly than at BDFFP: Trees in the 20 – 35 cm size class added an average of 0.047 ± 0.0057 MgC per MgC biomass, while the same sized trees in the BDFFP plots added 0.019 ± 0.0012 MgC per MgC biomass. These slower growth rates could lead to

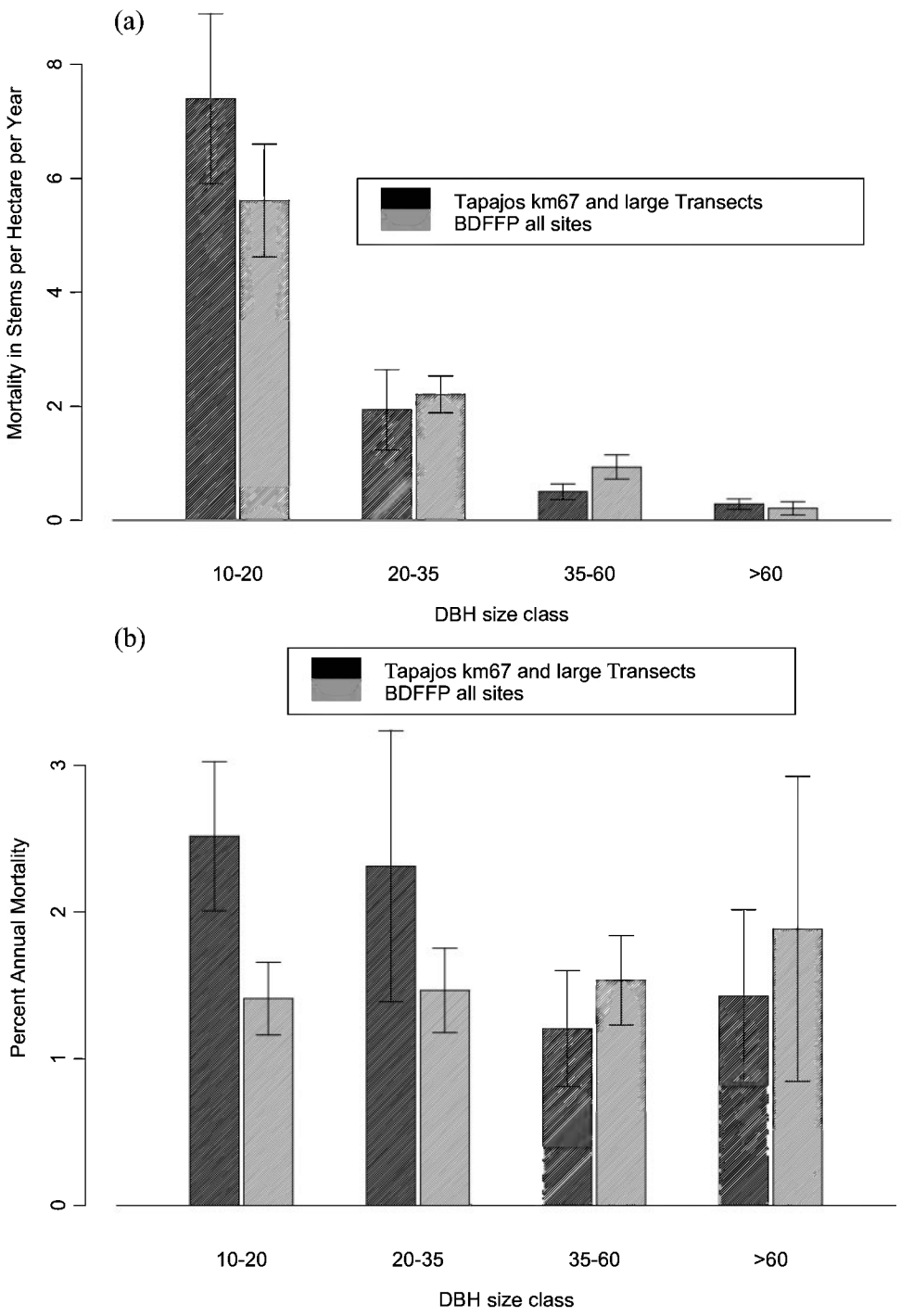

Figure 7. (a) Tree mortality by size class (tree ha^{-1} a^{-1}) for the TNF and BDFFP sites. Sites differ significantly ($p < 0.01$) only in the third size class, 35–60 cm DBH. (b) Proportional mortality (number of stems dying per year/live stem density) by size class. Sites differ significantly ($p < 0.01$) only in the first size class, 10–20 cm DBH. In Figures 7a and 7b, error bars show bootstrapped 95% confidence interval.

differences in age structure, where trees of the same size are older in Manaus: *Vieira et al.* [2005] found that tree ages average ~380 years in Manaus, but only average ~200–280 years in the TNF. This suggests that the greater dynamism at the TNF may be a long-established and ongoing phenomenon.

[42] Although the two sites show comparable overall mortality in terms of carbon lost from the pool of live biomass (Table 3), the total proportion of carbon in standing biomass lost through mortality is about 25% higher in the TNF. This site difference is reflected in the higher annualized mortality rates in the TNF (1.9% of stems in the TNF, 1.6% of stems in BDFFP), that suggest higher turnover rates

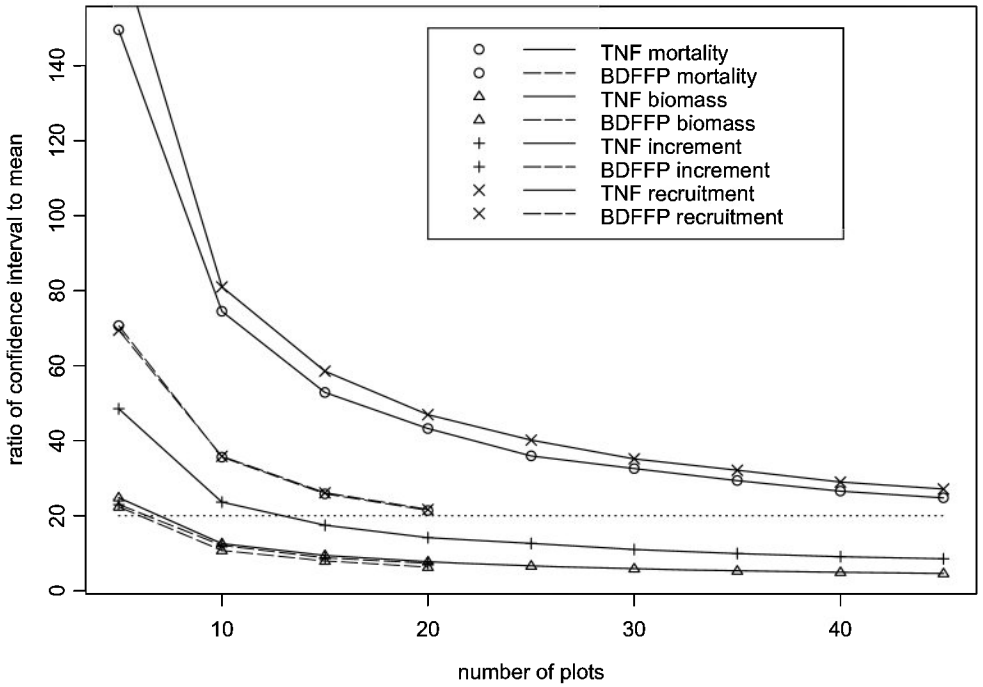

Figure 8. Subsampling in 1 ha plots at the TNF and BDFFP sites. Relationships between number of plots and "goodness" of estimate as measured by ratio of estimated mean to estimated confidence interval for mortality, biomass, growth increment, and recruitment. For mortality and recruitment, sites fell short of minimum ratio: for recruitment, TNF reached 26%, and BDFFP reached 22%; for mortality, TNF reached 24% and BDFFP reached 21%. Subsampling of smaller trees in TNF was incorporated in this simulated sampling analysis, where each 1 ha plot in the analysis represents 1 ha sample of trees > 35 cm DBH and an associated ~0.2 ha sample of trees > 10, <35 cm DBH. Total area sampled at BDFFP was 20 ha; total area sampled at TNF was 45 ha for trees > 35 cm DBH.

at TNF. Notably, the TNF showed higher stem mortality in the smallest size classes on both an absolute and per stem basis (Figure 7). The higher stem mortality in larger size classes in the BDFFP (Figure 7) leads to the equal estimates of overall carbon flux in mortality due to the weight of large trees in carbon estimates. In the TNF, higher mortality in the smallest trees may partially account for lower live tree stem counts and lower biomass in the small and middle size classes at the TNF. Higher mortality in the smallest size classes could be an underlying cause for the higher growth rates observed in the smallest size classes of TNF trees, and ultimately a driver of the higher overall turnover rates in the TNF, though because mortality is not are well constrained as other quantities, this possibility remains speculative.

[43] The higher mortality in small trees (<35 cm DBH) in the TNF could reflect the dominance of *Coussarea racemosa* A.Rich.ex.DC., a small-stature understory tree, which makes up 24% of trees <30 cm DBH at km 67, compared to <0.2% of trees <30 cm DBH in the BDFFP. *C.racemosa* tends to reach maximum size of ~30 cm DBH, and showed a 2.8% annual mortality from 2001 to 2005, 40% higher than the km 67 site average of ~2%a^{-1}. Understory trees typically have higher mortality rates than canopy trees [*Nascimento et al.*, 2005], but the prevalence of *C.racemosa* in particular might bias stem turnover for the smallest size classes at TNF.

[44] The forest in Manaus has shown evidence for seasonal water limitation in forest carbon flux [*Malhi et al.*, 2002; *Araújo et al.*, 2002], while the TNF has shown no signs of similar dry-season C uptake or evapotranspiration reductions due to water stress [*Hutyra et al.*, 2007; *Bruno et al.*, 2006] despite a longer dry season and lower annual rainfall at TNF. Continued dry season C uptake has been attributed to deep roots accessing deep water during dry season and thus maintaining a green and functioning canopy [*Nepstad et al.*, 1994]. Canopy carbon uptake at TNF increases late in the dry season [*Hutyra et al.*, 2007; *Goulden et al.*, 2004], possibly as a result of greater light availability and patterns in forest phenology [*Huete et al.*, 2006; *Saleska at al.*, 2007]. The combination of adequate water availability and a long, sunny dry season could be a factor contributing to the greater gross uptake in live biomass observed for the TNF, possibly driving higher mortality and turnover due to increased plant competition.

[45] Differences between TNF and BDFFP in size class structure appear to reflect differences in age structure, which in turn could result from differences in growth rates. It could be argued that the longer dry season at the TNF leads to greater carbon uptake in live trees, in turn leading to the stand structural differences observed in this study. Though the causality cannot be unambiguously attributed, due to the short period of study, the consistency among greater gross fluxes, greater carbon uptake in small trees, greater small tree mortality, and differences in stand and age distributions clearly indicate that the TNF is currently a more dynamic forest than the BDFFP.

5.2. Sampling Limitations and Spatial Pattern

[46] Our analysis of subplots showed the sampling of some demographic components of carbon flux was not quite adequate. Specifically, mortality and recruitment were not well sampled for either site (Figure 8, BDFFP: coefficient of variation for recruitment: 22%, for mortality: 21%; TNF: coefficient of variation for recruitment: 26%, for mortality: 24%) Much of the uncertainty around these demographic parameters in the TNF could have resulted from the subsampling of trees 10–35 cm DBH, the only size classes where recruitment occurs and important sizes classes for mortality. Notably, the much larger sampling area for small trees in the BDFFP (more than double, with 20 ha versus ~8.5 ha in the TNF) reduced the coefficient of variation by only a few percentage points (3–4%), suggesting the inherent difficulty in adequately sampling these dynamic demographic quantities. The episodic nature of mortality and the influence of individual large tree deaths on individual subplots likely complicate such estimates.

[47] Though mortality and recruitment fluxes may not be as well constrained as other fluxes in this study, they exert less influence on the overall estimates of net flux of carbon in forest biomass. With mortality, the flux of biomass from the pool of live biomass to CWD (mortality) does not factor into the net flux (growth + recruitment – CWD respiration). With recruitment, the flux of carbon into the pool of live biomass due to recruitment is ~10% of the total flux of carbon into biomass for both sites, with the remaining ~90% due to growth of live trees, which is well sampled.

[48] Another potential problem in the subplots analysis for the TNF is that the locations of individual 1 ha subplots in the TNF were constrained by the configuration of randomly located transects, unlike the stratified random placement of the individual BDFFP plots. The spatial constraints on TNF subplots could lead to spatial autocorrelation; however, our analysis of distance and similarity showed no signs of spatial trends in the measured forest quantities: plots located in close proximity were not more similar. Moreover, if TNF subplots were auto-correlated, they would be more likely to show lower variability: the reverse of what we found.

[49] Subplots were also used for spatial analysis which showed no pattern of variation at the scale of 1–50 km: Plots located in close proximity showed the same range of similarities (mean squared difference) as plots separated by larger distances. While there may be fine scale spatial variability in carbon dynamics (e.g., gap dynamics), these processes do not appear to influence variability at the landscape scale; i.e., there are not some areas more prone to tree falls or other sources of fine scale variability at the landscape scale (~1 to ~50 km). This consistency within both sites suggests that a localized patch of sampling (of adequate size) can provide a reasonable estimate of the larger matrix of forest on the 50 km scale; i.e., the research plots at km 67 do characterize biomass for terra firme forest in the TNF in general, and an eddy flux tower "foot print" may be considered representative of the surrounding forest. It is important to note, however, that by design, plots in this study did not sample across obvious topological or edaphic gradients, where landscape scale spatial variation might be apparent, and thus an adequate local sample may not reflect the surrounding forest where there are notable shifts in forest type or conditions.

[50] The differences between the two sites, TNF and BDFFP were consistent, possibly due in part to low internal variability within each site discussed above. This spatial consistency indicates that the factors regulating the site differences act across the landscape scale and over sufficiently long time periods to shape both stand structural qualities and dynamics. Such forest-wide causes of site differences may include climatological, edaphic, and/or meteorological conditions. In the BDFFP area, the poor quality of weathered, acidic soils, or the dissected terrain might limit tree growth rates and favor denser, slower growing species in the forest outside of Manaus [*Nascimento et al.*, 2005; *Vieira et al.*, 2005]. While the larger gross fluxes in live biomass growth and CWD decomposition in the TNF may reflect influences of soils, climate regime, topology, they are most clearly linked to disturbance and recovery. The strong signal of disturbance recovery and disequilibrium detected in the TNF defines the carbon dynamics observed there and cannot be separated from other, long-term influences on carbon balance.

5.3. Disequilibria, Disturbance, and the Importance of CWD

[51] At both sites, CWD plays a pivotal role in ecosystem carbon dynamics and is a key indicator of underlying causes of site differences. CWD stocks at both the TNF and BDFFP led to a significant shift in the observed net carbon balance: without consideration of the CWD pools the data show moderate (~0.8 $MgC \bullet ha^{-1} \bullet a^{-1}$) uptake in the TNF and small uptake (~0.3 $MgC \bullet ha^{-1} \bullet a^{-1}$) in the BDFFP plots (Figure 6, left hand bars only), leading to the conclusion that both sites are net storing carbon in biomass [cf. *Vieira et al.*, 2004; *Baker et al.*, 2004]. This result would seem to support the conclusion that sequestration of carbon is widespread in Amazonian forests [cf. *Baker et al.*, 2004; *Phillips et al.*, 2002]. But inclusion of the CWD carbon flux turned the TNF into a significant net source (-1.25 ± 0.45 $MgC \bullet ha^{-1} \bullet a^{-1}$) and changed the carbon balance from a small sink to carbon neutral (0.18 ± 0.29 $MgC \bullet ha^{-1} \bullet a^{-1}$) for the BDFFP. Moreover, with CWD included, land-based measurements more closely matched the tower-based NEE measurements in TNF, which indicated a small source transitioning to neutral between 2001 and 2005 [*Hutyra et al.*, 2008, Table 3].

[52] Site comparisons of CWD could be complicated by the differences in wood density and decay classifications. In the case of this study, the decay classes used in the BDFFP study did not precisely match those used in the TNF study, but they were consistent. For example, the density values of the "sound" decay class used in the BDFFP sites (0.69 $Mg \bullet m^{-3}$), falls between the density values used in the TNF for decay classes 1 and 2 (0.60, and 0.70 $Mg \bullet m^{-3}$, respectively). Site-specific densities applied for each site may be the most appropriate choice where CWD wood density varies spatially [*Chao et al.*, 2008]. Though the compatibility of the size class and densities applied at each site cannot be tested with the data available, the efficacy of the CWD methods for each site is supported by independent estimates. The BDFFP estimate (~16 $MgC \bullet ha^{-1}$) concurs with that of *Summers* [1998] (~15 $MgC \bullet ha^{-1}$) who directly

Table 4. Values for Carbon Pool and Fluxes by Size Class Used to Build Box Model for the TNF and the BDFFP Sites[a]

Class	Mass ($MgC \bullet ha^{-1}$)	Growth Within Size Class ($MgC \bullet ha^{-1} \bullet a^{-1}$)	Growth Into Size Class ($MgC \bullet ha^{-1} \bullet a^{-1}$)	Mortality ($MgC \bullet ha^{-1} \bullet a^{-1}$)	Respiration Rate (a^{-1})	Net Change ($MgC \bullet ha^{-1} \bullet a^{-1}$)
			TNF			
B1 10–20 cm DBH	21.03 ± 0.35	0.79 ± 0.038	0.48 ± 0.021 (recruitment)	0.45 ± 0.047	-	0.08 ± 0.081
B2 20–35 cm DBH	30.03 ± 0.70	0.84 ± 0.079	0.74 ± 0.048	0.62 ± 0.09	-	−0.33 ± 0.16
B335–60 cm DBH	42.67 ± 0.53	0.81 ± 0.045	1.29 ± 0.10	0.53 ± 0.063	-	0.74 ± 0.14
B4 >60 cm DBH	60.80 ± 1.16	0.40 ± 0.040	0.83 ± 0.066	1.01 ± 0.12	-	0.22 ± 0.15
CWD	43.9 ± 5.06	-	-	-	0.123 ± 0.0001	−2.8 ± 0.64
			BDFFP			
B1 10–20 cm DBH	24.82 ± 0.30	0.52 ± 0.018	0.25 ± 0.008 (recruitment)	0.33 ± 0.016	-	−0.16 ± 0.21
B2 20–35 cm DBH	48.55 ± 0.71	0.81 ± 0.041	0.60 ± 0.12	0.70 ± 0.040	-	−0.17 ± 0.33
B3 35–60 cm DBH	65.84 ± 1.18	0.74 ± 0.060	0.88 ± 0.24	1.00 ± 0.068	-	0.28 ± 0.29
B4 >60 cm DBH	27.35±1.15	0.19±0.040	0.32±0.19	0.54±0.077	-	−0.03±0.21
CWD	16.2 ± 1.15	-	-	-	0.123 ± 0.0001	0.58 ± 0.13

[a]Errors are 95% confidence intervals calculated by bootstrap analysis.

estimated CWD in 3, 1 ha plots only 20 km south of the BDFFP area. Likewise, the TNF CWD estimate (~40 $MgC \bullet ha^{-1}$) is similar to the estimate provided by *Palace et al.* [2007] (~41 $MgC \bullet ha^{-1}$) for trees ≥ 10 cm DBH in unlogged forest near km 83 in the TNF.

[53] Diagnosis of the factors controlling CWD cannot, unfortunately, be inferred just from measurements of the CWD pool. The CWD distribution between standing and downed trees, which might be expected to provide an indication of disturbance mechanisms (blow-downs versus standing dead), was variable at both sites over a similar range (10–30%), likely a reflection of the high variability of both mortality and disturbance in space, time and intensity. *Rice et al.* [2004] found standing to be 18% (8.6 $MgC \cdot ha^{-1}$) of CWD; *Clark et al.* [2002] found 12% (3.1 $MgC \cdot ha^{-1}$); *Palace et al.* [2007] report standing CWD ranged from 12 to 17% of total, depending on site and treatment (some sites had experienced reduced impact logging). This consistent variability across sites indicates that the proportion of standing CWD is not a good indicator of site differences or causes of mortality.

[54] The mortality rates measured over the study period were also comparable in terms of carbon lost from the pool of live biomass, though the TNF mortality was proportionally higher by stem count (1.9% in the TNF, 1.6% in BDFFP). The TNF mortality was not high enough, however, to account for the much larger CWD pool at the TNF. The very large stock of CWD distributed throughout the TNF must have resulted from excessive (higher than current observations) mortality occurring at our measurement sites in the TNF before the start of the study. Strong drought conditions were measured in the region of the TNF during the 1997–98 ENSO event, and *Rice et al.* [2004] proposed that this drought could have produced a mortality pulse leading to the imbalance in CWD observed at km 67 in 1999–2001. In the BDFFP plots, *Williamson et al.* [2000] documented increased mortality rates during the 1997–1998 ENSO, though the CWD pools in the BDFFP plots do not show excess CWD or a residual imbalance during the time period of this study. However, the magnitude of the mortality increase reported for BDFFP plots (from 1.12% – 1.91%) was considerably smaller than other reported ENSO-related mortality increases (2–3% [*Condit et al.*, 1995]) [*Leighton and Wirawan*, 1986]. See review in *Clark* [2004b, Table 1]. While there are no tree mortality data for the TNF during the time period of the ENSO, *Rice et al.* [2004] estimated that mortality of roughly 5% of the standing biomass, persisting for 5 years, would be required to yield the excess CWD found in the TNF in 2001.

[55] Another possible source for excessive CWD could include nonfatal limb and branch falls which contribute to the CWD, but would not be accounted for with mortality-derived estimates of CWD inputs [*Rice et al.*, 2004; *Chambers et al.*, 2001a]. *Palace et al.* [2007] found that using mortality rates to estimate coarse wood production underestimates CWD production by 30–50%, based on direct measurements of coarse wood inputs in the TNF. In this study, CWD values were limited to ≥10 cm, a minimum size that may exclude many limb falls. *Palace et al.* [2007] reported a coarse wood production value for large pieces (≥10 cm) of 4.7 $Mg \bullet ha^{-1} \bullet a^{-1}$, slightly lower than our mortality derived estimate of 5.2 $Mg \bullet ha^{-1} \bullet a^{-1}$, suggesting we have not underestimated the inputs into our pool of CWD.

[56] Our linearized box model, based on Figure 2, further illuminates disequilibria of the biomass pools at TNF. Figure 2 provides a quantitative visualization of the mass balances of the major stocks of organic matter at the two sites. At TNF, only the smallest size class was approximately in steady state, with total inputs (recruitment + growth in class = 1.27 $MgC \bullet ha^{-1} \bullet a^{-1}$) approximately balancing outputs (export + mortality = 1.19 $MgC \bullet ha^{-1} \bullet a^{-1}$; net flux 0.08 ± 0.08 $MgC \bullet ha^{-1} \bullet a^{-1}$; see Table 4). The second size class experienced strong growth, but exported more biomass to the next larger class than it retained. The two largest size classes grew at significant rates, and the CWD pool declined rapidly (~6%$\bullet a^{-1}$). In contrast, at BDFFP, the live biomass stocks were each close to being in balance (within error), and the CWD pool may have been accumulating at a slow rate. The apparent imbalances in each size class indicate that the structure of the forest at the TNF was shifting significantly at the time of measurement, while the BDFFP was much closer to a steady condition. The differences shown for the net fluxes of the major pools belie the similarity that might have been expected given the comparable totals of biomass.

[57] If we imagine that the system evolves forward and backward in time with fixed transition and growth frequen-

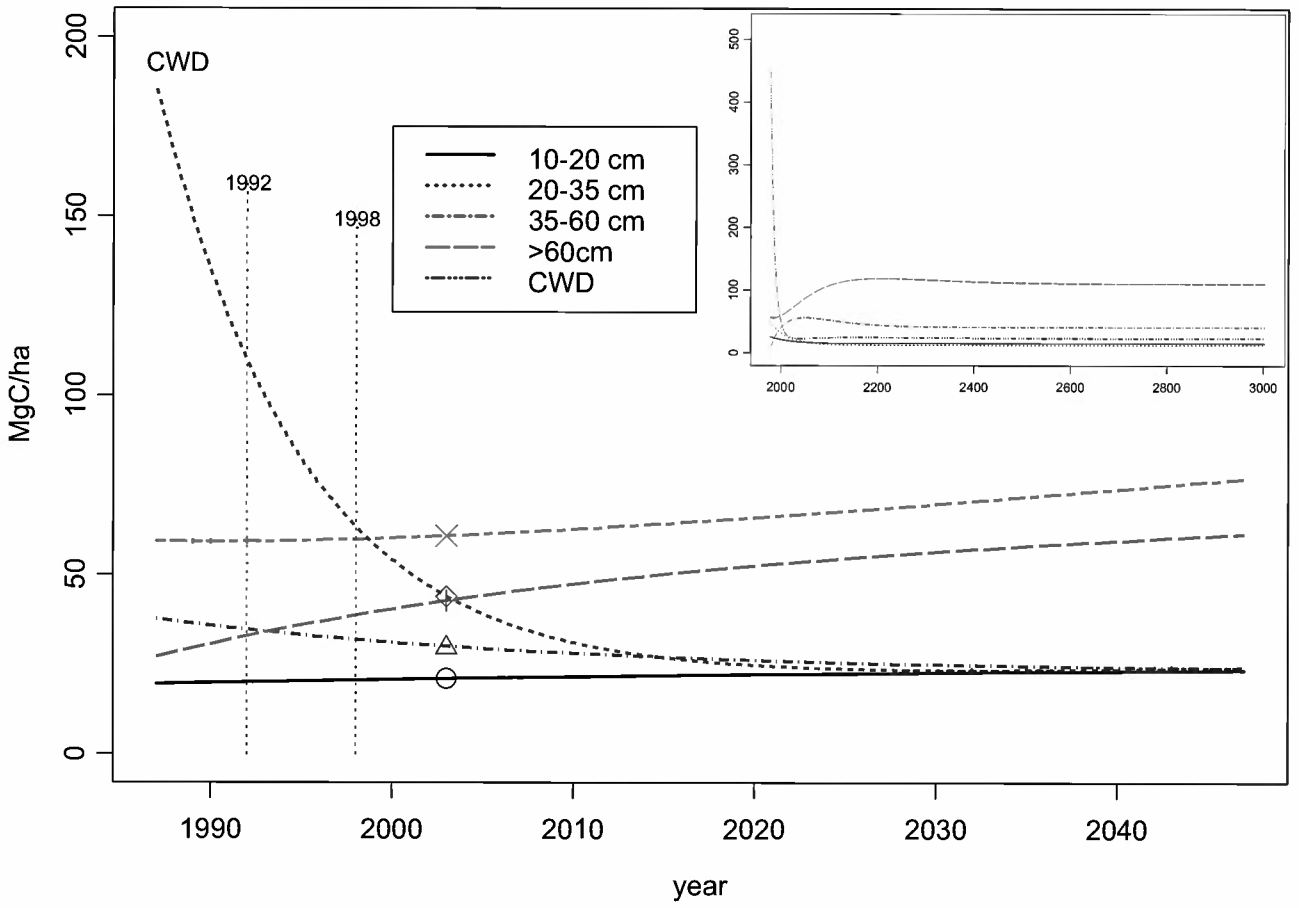

Figure 9. Modeled trajectories of carbon in different size classes of live trees and CWD for the TNF. Results from box model show short-term reduction of the CWD pool followed by long-term accrual of carbon in forest biomass (inset). Symbols mark the baseline values from 2003 used to construct the model.

cies, the box model can also be used to place a bound on the date for a mortality pulse by computing the date back in time where the modeled CWD pool would become "excessive" or not biologically possible. If the pulse of excess mortality had occurred as long ago as 1992, the initial CWD pool would have to have been 90.3 MgC·ha^{-1}, equivalent to ~38% total woody biomass (Figure 9). A CWD pool of this magnitude would imply an input pulse of ~60 MgC·ha^{-1}, or 25% of standing biomass, representing a major, visible die-off of the forest. If the CWD increase happened in 1998, the CWD pool would have been 54 MgC·ha^{-1} (~26% total woody biomass), implying an input of > 20 MgC·ha^{-1} provided by excess mortality. This input would correspond to ~10% mortality or about 7 times the rate observed during the nondrought years of our observations, a mortality level comparable to the total mortality observed in the 3-year drydown experiment of *Nepstad et al.* [2007] in the TNF.

[58] Drought could also contribute to a CWD increase by inhibiting decomposition rates due to moisture limitations [*Rice et al.*, 2004]. Several studies have shown lower ecosystem respiration with seasonally dry conditions at TNF [*Goulden et al.*, 2004; *Davidson et al.*, 2004; *Saleska et al.*, 2003].

[59] The large pool of CWD remained unbalanced in the TNF through the 6 years of this study, though the magnitude of the C imbalance for at km 67 diminished in the 2001 to 2005 interval, relative to the 1999 to 2001 interval (Figure 6a), confirmed by eddy flux data that showed NEE approaching zero. Increased mortality (2.87 MgC•ha^{-1}•a^{-1}) at km 67 from 2001 to 2005 offset the reduction of the CWD pool via CWD respiration (4.84 MgC•ha^{-1}•a^{-1}), while large-scale transects T3 and T6 showed lower mortality (2.4 and 2.1 MgC•ha^{-1}•a^{-1}, respectively), and edged closer to overall carbon balance, with error bars spanning zero in some cases (Figure 6a).

[60] How much longer could the imbalance in the TNF last? Using a simple model of CWD respiration at km 67 [*Hutyra et al.*, 2008] and assuming tree growth and recruitment rate constants remain constant, we estimate that the CWD pool could be reduced to the point where CWD respiration would be matched by growth and recruitment of live biomass sometime in 2011 (Figure 9), perhaps a bit earlier [2007] if mortality were lower than observed at km 67 from 2001 to 2005. The continued CWD imbalance in this study suggests that carbon release following a disturbance could last as long as 10–15 years.

[61] Note that near equilibration of the CWD pool in 2007–2011 indicated in Figure 9 does not imply that the TNF will reach a steady state in that time. The simple model has eigenvalues corresponding to time scales λ = 8.1, 28, 52, 77, and 100 years. The decay rate of CWD fixes the shortest time scale but adjustments among the size classes

take much longer (Figure 9, inset): tree boles decay faster than they are constructed. Moreover, the model assumes continuation of current fluxes, which could change with changing environmental conditions or disturbance.

5.4. Implications and Conclusions

[62] The measurements reported here of fluxes between major stocks of biomass, and complementary eddy flux data provide a strong foundation for quantitatively defining the factors regulating carbon stocks and fluxes in these Amazonian forests. We found significant differences between two sites in the central and eastern Amazon, with TNF showing notably larger gross fluxes in live and dead biomass than the BDFFP plots. Major carbon pools were close to steady state in the BDFFP plots, but significantly out of equilibrium at TNF. Disequilibrium was found on multiple levels in the TNF, with a large CWD imbalance and significant shifting in live tree size class structure. The stand structural changes represent a legacy that, based on observed imbalances and comparison with BDFFP data, will tend to persist for over a decade.

[63] Legacies of probable disturbance were captured and quantified in the measurements at TNF and our analysis shows the TNF responding rapidly to apparent disturbance by releasing carbon to the atmosphere. Our box model predicts that this release will be short (~10 years) and followed by an extended period of uptake and adjustments of forest structure, in the absence of a major disturbance. Our data quantify, at the landscape scale, the phenomena of disturbance—recovery widely discussed in the absence of such data hitherto [e.g., *Körner*, 2004; *Clark*, 2004a; *Moorcroft et al.*, 2001].

[64] This analysis of two sites showing disparate carbon dynamics does not allow estimation of the net carbon balance of the entire Amazon Basin. While our two sites are internally consistent in carbon balance, the way they fit into the basin as a whole remains unknown. *Baker et al.* [2007] suggested some sites in the Western Amazon are close to equilibrium, with low CWD and no signs of recent disturbance. Most likely, the sites in this study represent points in a continuum of disturbance-recovery cycles, where the TNF carbon dynamics presented here exemplify carbon dynamics of more recently disturbed sites. The long-term balance of the Amazon Basin will be determined by the abundance and longevity of sites within this disturbance-recovery continuum: carbon accumulation at a majority of sites may be more than compensated for by episodic release of CO_2 during and shortly after major disturbances. Indeed, two recent studies have reported a majority of forest inventory plots showing accumulation of live biomass along with infrequent plots showing excessive biomass loss [*Feeley et al.*, 2007; *Chave et al.*, 2008]. To assess trends in Basin-wide carbon balance, we require further observations (remote sensing, eddy covariance, biometric, etc.) that can accurately detect, over large areas for long times, the ensemble of mortality events that involve single trees or small groups of trees.

[65] **Acknowledgments.** This research was part of the Brazil-led Large Scale Biosphere-atmosphere Experiment in Amazonia, funded primarily through the NASA grants NCC5-341, NCC5-684, and NNG06GG69A to Harvard University. It was also made possible by the Harvard University Center for the Environment, the Harvard College Research Fund, and Harvard University's David Rockefeller Center for Latin American Studies. We would like to thank the team at the LBA-Santarém Office: Bethany Reed, Lisa Merry, Dan Hodkinson, and Michael Keller (Director), for their logistical support; Kadson Silva, Dulcyana Ferreira, Raimundo Lima, Jadson Dizencourt Dias, Marcello da Silva Feitosa, and the other members of the CD-10 team for their help in both the field and in the office; Nilson de Souza Carvalho and Ehrly Pedroso for their knowledge and dedication in the field; and Josias Freitas, Itamar, Chieno for their assistance in the field; Daniel Jacob, Paul Moorcroft, and Bill Munger for advice on analyses for various versions of this paper. For the Biological Dynamics of Forest Fragments Project, funding was provided by the NASA/LBA Program; Programa Piloto para Proteção das Florestas Tropicais (PPG-7); A. W. Mellon Foundation; Conservation, Food, and Health Foundation; World Wildlife Fund-U.S.; MacArthur Foundation; National Institute for Amazonian Research (INPA); Fundaço de Amaparo à Pesquisa do Amazonas (FAPEAM); Conselho Nacional de Desenvolvimento Cientuacute;fico e Tecnológico (CNPq); and Smithsonian Institution (SI). This is the publication 510 in the BDFFP technical series.

References

Adams, J. M., and G. Piovesan (2005), Long series relationships between global interannual CO2 increment and climate: Evidence for stability and change in role of the tropical and boreal-temperate zones, *Chemosphere*, *59*, 1595–1612, doi:10.1016/j.chemosphere.2005.03.064.

Araújo, A. C., et al. (2002), Comparative measurements of carbon dioxide fluxes from two nearby towers in a central Amazonian rainforest: The Manaus LBA site, *J. Geophys. Res.*, *107*(D20), 8090, doi:10.1029/2001JD000676.

Baker, T. R., et al. (2004), Variation in wood density determines spatial patterns in Amazonian forest biomass, *Global Change Biol.*, *10*, 545–562, doi:10.1111/j.1365-2486.2004.00751.x.

Baker, T. R., E. N. H. Coronado, O. L. Phillips, J. Martin, G. M. F. van der Heijden, M. Garcia, and J. S. Espejo (2007), Low stocks of coarse woody debris in a southwest Amazonian forest, *Oecologia*, doi:10.1007/s00442-007-0667-5.

Barford, C. C., S. C. Wofsy, M. L. Goulden, J. W. Munger, E. H. Pyle, S. P. Urbanski, L. Hutyra, S. R. Saleska, D. Fitzjarrald, and K. Moore (2001), Factors controlling long- and short-term sequestration of atmospheric CO_2 in a mid-latitude forest, *Science*, *294*, 1688–1691, doi:10.1126/science.1062962.

Bosquet, P., P. Peylin, P. Ciais, C. Le Quere, P. Friedlingstein, and P. P. Tans (2000), Regional changes in carbon dioxide fluxes of land and oceans since 1980, *Science*, *290*, 142–144, doi:10.1126/science.290.5489.142.

Brown, J. K. (1974), Handbook for inventorying downed woody material, general technical report, U. S. Dep. of Agric. For. Serv., Ogden, Utah.

Brown, S. (1997), Estimating biomass and biomass change of tropical forests: A primer, 55 pp. U. N. Food and Agric. Org., Urbana, Ill.

Bruno, R. D., H. R. da Rocha, H. C. de Freitas, M. L. Goulden, and S. D. Miller (2006), Soil moisture dynamics in an eastern Amazonian tropical forest, *Hydrol. Process.*, *20*, 2477–2489, doi:10.1002/hyp.6211.

Carswell, F. E., et al. (2002), Seasonality in CO_2 and H_2O flux at an eastern Amazonian rain forest, *J. Geophys. Res.*, *107*(D20), 8076, doi:10.1029/2000JD000284.

Chambers, J. Q., N. Higuchi, L. V. Ferreira, J. M. Melack, and J. P. Schimel (2000), Decomposition and carbon cycling of dead trees in tropical forests of the central Amazon, *Oecologia*, *122*, 380–388, doi:10.1007/s004420050044.

Chambers, J. Q., J. dos Santos, R. J. Ribiero, and N. Higuchi (2001a), Tree damage, allometric relationships, and aboveground net primary production in a central rainforest, *For. Ecol. Manage.*, *152*, 73–84, doi:10.1016/S0378-1127(00)00591-0.

Chambers, J. Q., J. P. Schimel, and A. D. Nobre (2001b), Respiration from coarse wood litter in central Amazonian forests, *Biogeochemistry*, *52*, 115–131, doi:10.1023/A:1006473530673.

Chambers, J. Q., N. Higuchi, L. M. Teixeira, J. dos Santos, S. G. Laurance, and S. E. Trumbore (2004), Response of tree biomass and wood litter to disturbance in a central Amazon forest, *Oecologia*, *141*, 596–611doi:10.1007/s00442-004-1676-2.

Chao, K.-J., O. L. Phillips, and T. R. Baker (2008), Wood density and stocks of coarse woody debris in a northwestern Amazonian landscape, *Can. J. For. Res.*, *38*doi:10.1139/X07-163.

Chave, J., R. Condit, S. Lao, J. P. Caspersen, R. B. Foster, and S. P. Hubbell (2003), Spatial and temporal variation of biomass in a tropical forest: Results from a large census plot in Panama, *J. Ecol.*, *91*, 240–252, doi:10.1046/j.1365-2745.2003.00757.x.

Chave, J., et al. (2005), Tree allometry and improved estimation of carbon stocks and balance in tropical forests, *Oecologia*, *145*, 87–99, doi:10.1007/s00442-005-0100-x.

Chave, J., H. C. Muller-Landau, T. R. Baker, T. A. Easdale, H. ter Steege, and C. O. Webb (2006), Regional and phylogenetic variation of wood

density across 2456 neotropical tree species, *Ecol. Appl.*, *16*, 2356–2367, doi:10.1890/1051-0761(2006)016[2356:RAPVOW]2.0.CO;2.

Chave, J., et al. (2008), Assessing evidence for a pervasive alteration in tropical tree communities, *PLoS Biol.*, *6*(3), e45, doi:10.1371/journal.pbio.0060045.

Clark, D. A. (2004a), Tropical forests and global warming: Slowing it down or speeding it up?, *Front. Ecol. Environ*, *2*, 71–80.

Clark, D. A. (2004b), Sources of sinks? The responses of tropical forests to current and future climate and atmospheric composition, *Philos. Trans. R. Soc. London, Ser. B*, *359*, 477–491, doi:10.1098/rstb.2003.1426.

Clark, D. A., S. Brown, D. W. Kicklighter, J. Q. Chambers, J. R. Thomlinson, J. Ni, and E. A. Holland (2001a), Net primary production in tropical forests: An evaluation and synthesis of existing field data, *Ecol. Appl.*, *11*, 371–384, doi:10.1890/1051-0761(2001)011[0371:NPPITF]2.0.CO;2.

Clark, D. A., S. Brown, D. W. Kicklighter, J. Q. Chambers, J. R. Thomlinson, and J. Ni (2001b), Net primary production in tropical forests: Concepts and field methods, *Ecol. Appl.*, *11*, 356–370, doi:10.1890/1051-0761(2001)011[0356:MNPPIF]2.0.CO;2.

Clark, D. A., S. C. Piper, C. D. Keeling, and D. B. Clark (2003), Tropical rain forest tree growth and atmospheric carbon dynamics linked to interannual temperature variation during 1984–2000, *Proc. Natl. Acad. Sci.*, *100*, 5852–5857, doi_10.1073_pnas.0935903100.

Clark, D. B., and D. A. Clark (2000), Landscape-scale variation in forest structure and biomass in a tropical rain forest, *For. Ecol. Manage.*, *137*, 185–198, doi:10.1016/S0378-1127(99)00327-8.

Clark, D. B., D. A. Clark, S. Brown, S. F. Oberbauer, and E. Veldkamp (2002), Stocks and flows of coarse woody debris across a tropical rain forest nutrient and topography gradient, *For. Ecol. Manage.*, *164*, 237–248, doi:10.1016/S0378-1127(01)00597-7.

Condit, R. S., S. P. Hubbell, and R. B. Foster (1995), Mortality rates of 205 Neotropical tree and shrub species and the impact of a severe drought, *Ecol. Monogr.*, *65*, 419–439, doi:10.2307/2963497.

Cummings, D. L., J. B. Kauffman, D. A. Perry, and R. F. Hughes (2002), Aboveground biomass and structure of rainforests in the southwestern Brazilian Amazon, *For. Ecol. Manage.*, *163*, 293–307, doi:10.1016/S0378-1127(01)00587-4.

Davidson, E. A., F. Y. Ishida, and D. C. Nepstad (2004), Effects of and experimental drought on soil emissions of carbon dioxide, methane, nitrous oxide, and nitric oxide in a moist tropical forest, *Global Change Biol.*, *10*, 718–730, doi:10.1111/j.1365-2486.2004.00762.x.

de Castilho, C. V., W. E. Magnusson, R. N. O. deAraújo, R. C. C. Luizão, A. P. Lima, and N. Higuchi (2006), Variation in aboveground tree live biomass in a central Amazonian forest: Effects of soil and topography, *For. Ecol. Manage.*, *234*, 85–96, doi:10.1016/j.foreco.2006.06.024.

Delaney, M., S. Brown, A. E. Lugo, A. Torres-Lezama, and N. B. Quintero (1998), The quantity and turnover of dead wood in permanent forest plots in six life zones of Venezuela, *Biotropica*, *30*, 2–11, doi:10.1111/j.1744-7429.1998.tb00364.x.

de Oliveria, A. A., and S. A. Mori (1999), A central Amazonian terra firme forest. I. High tree species richness on poor soils, *Biodivers. Conserv.*, *8*, 1219–1244, doi:10.1023/A:1008908615271.

Efron, B., and R. J. Tibshirani (1993), *An Introduction to the Bootstrap*, 436 pp., Chapman and Hall, New York.

Fearnside, P. M. (1997), Wood density for estimating forest biomass in Brazilian Amazonia, *For. Ecol. Manage.*, *90*, 59–87doi:10.1016/S0378-1127(96)03840-6.

Feeley, K. J., S. J. Davies, P. S. Ashton, S. Bunyavejchewin, M. N. Nur Supardi, A. R. Kassim, S. Tan, and J. Chave (2007), The role of gap phase processes in the biomass dynamics of tropical forests, *Proc. R. Soc. London, Ser. B*, *274*, 2857–2864, doi:10.1098/rspb.2007.0954.

Field, C. B., M. J. Behrenfeld, J. T. Randerson, and P. Falkowski (1998), Primary production of the biosphere: Integrating terrestrial and oceanic components, *Science*, *281*, 237–240, doi:10.1126/science.281.5374.237.

Food and Agriculture Organization (FAO) (1993), *Third interim report on the state of tropical forests*, Rome.

Goulden, M. L., S. D. Miller, H. R. da Rocha, M. C. Menton, H. C. Freitas, A. M. Figueira, and A. C. D. de Sousa (2004), Diel and seasonal patterns of tropical forest CO_2 exchange, *Ecol. Appl.*, *14*, 42–54, doi:10.1890/02-6008.

Harmon, M. E., and J. Sexton (1996), Guidelines for measurements of woody debtritus in forest ecosystems, Publ. *20*, 73 pp., U. S. LTER Network Off., Univ. of Wash., Seattle.

Houghton, R. A. (2005), Aboveground Forest biomass and the global carbon balance, *Global Change Biol.*, *11*, 945–958, doi:10.1111/j.1365-2486.2005.00955.x.

Huete, A. R., K. Didan, Y. E. Shimabukuro, P. Ratana, S. R. Saleska, L. R. Hutyra, W. Yang, R. R. Nemani, and R. Myeni (2006), Amazon rainforests green-up with sunlight in dry season, *Geophys. Res. Lett.*, *33*, L06405, doi:10.1029/2005GL025583.

Hurlbert, S. H. (1984), Pseudoreplication and the design of ecological field experiments, *Ecol. Monogr.*, *54*, 187–211, doi:10.2307/1942661.

Hutyra, L. R., J. W. Munger, S. R. Saleska, E. Gottlieb, B. C. Daube, A. L. Dunn, D. F. Amaral, P. B. de Camargo, and S. C. Wofsy (2007), Seasonal controls on the exchange of carbon and water in an Amazonian rain forest, *J. Geophys. Res.*, *112*, G03008, doi:10.1029/2006JG000365.

Hutyra, L. R., J. W. Munger, E. H. Pyle, S. R. Saleska, N. Restrepo-Coupe, P. B. de Camargo, and S. C. Wofsy (2008), Resolving systematic errors in estimates of net ecosystem exchange of CO_2 and ecosystem respiration in a tropical forest biome, *Agric. For. Meteorol.*, doi:10.1016/j.agrformet.2008.03.007, in press.

Keller, M., M. Palace, and G. Hurtt (2001), Biomass estimation in the TNF, Brazil: Examination of sampling and allometric uncertainties, *For. Ecol. Manage.*, *154*, 371–382, doi:10.1016/S0378-1127(01)00509-6.

Körner, C. (2004), Through enhanced tree dynamics carbon dioxide enrichment may cause tropical forests to lose carbon, *Philos. Trans. R. Soc. London, Ser. B*, *359*, 493–498, doi:10.1098/rstb.2003.1429.

Laurance, W. F., P. M. Fearnside, S. G. Laurance, P. Delamonica, T. E. Lovejoy, J. M. Rankin-de-Merona, J. Q. Chambers, and C. Gascon (1999), Relationship between soils and Amazon forest biomass: A landscape-scale study, *For. Ecol. Manage.*, *118*, 127–138, doi:10.1016/S0378-1127(98)00494-0.

Laurance, W. F., T. E. Lovejoy, H. L. Vasconcelos, E. M. Bruna, R. K. Didham, P. C. Stouffer, C. Gascon, R. O. Bierregaard, S. G. Laurance, and E. Sampaio (2002), Ecosystem decay of Amazonian forest fragments: A 22-year investigation, *Conserv. Biol.*, *16*(3), 605–618, doi:10.1046/j.1523-1739.2002.01025.x.

Leighton, M., and N. Wirawan (1986), Catastrophic drought and fire in Borneo tropical rainforest associated with the 1982–83 El Niño Southern Oscillation event, in *Tropical Rain Forests and the World Atmosphere*, edited by G. T. Prance pp. 75–102, Westview, Boulder, Colo.

Lovejoy, T. E., et al. (1986), Edge and other effects of isolation on Amazon forest fragments, in *Conservation Biology: The Science of Scarcity and Diversity*, edited by M. E. Soulé, pp 257–285, Sinauer, Sunderland, Mass.

Malhi, Y., A. D. Nobre, J. Grace, B. Kruijt, M. G. P. Pereira, A. D. Culf, and S. Scott (1998), Carbon dioxide transfer over a Central Amazonian rain forest, *J. Geophys. Res.*, *103*, 31,593–31,612.

Malhi, Y., E. Pegoraro, A. D. Nobre, M. G. P. Pereira, J. Grace, A. D. Culf, and R. Clement (2002), Energy and water dynamics of a central Amazonian rain forest, *J. Geophys. Res.*, *107*(D20), 8061, doi:10.1029/2001JD000623.

Malhi, Y., et al. (2004), The above-ground coarse wood productivity of 104 neotropical forest plots, *Global Change Biol.*, *10*, 563–591, doi:10.1111/j.1529-8817.2003.00778.x.

Malhi, Y., et al. (2006), The regional variation of aboveground live biomass in old-growth Amazonian forests, *Global Change Biol.*, *12*, 1107–1138, doi:10.1111/j.1365-2486.2006.01120.x.

Miller, S. D., M. L. Goulden, M. C. Menton, H. R. da Rocha, H. C. de Freitas, A. M. E. Figueira, and C. A. D. de Sousa (2004), Biometric and micrometeorological measurements of tropical forest carbon balance, *Ecol. Appl.*, *14*, 114–126, doi:10.1890/02-6005.

Moorcroft, P. R., G. C. Hurtt, and S. W. Pacala (2001), A method for scaling vegetation dynamics: The ecosystem demography model, *Ecol. Monogr.*, *71*, 557–586.

Nascimento, H. E. M., and W. F. Laurance (2002), Total aboveground biomass in central Amazonian rainforests: A landscape-scale study, *For. Ecol. Manage.*, *168*, 311–321, doi:10.1016/S0378-1127(01)00749-6

Nascimento, H. E. M., W. F. Laurance, R. Condit, S. G. Laurance, S. D'Angelo, and A. C. Andrade(2005), Demographic and life-history correlates for Amazonian trees, *J. Veg. Sci.*, *16*, 625–634, doi:10.1658/1100-9233(2005)016[0625:DALCFA]2.0.CO;2

Nepstad, D. C., C. R. de Carvalho, E. A. Davidson, P. H. Jipp, P. A. Lefebvre, G. H. Negreiros, E. D. da Silva, T. A. Stone, S. E. Trumbore, and S. Vieira (1994), The role of deep roots in the hydrological and carbon cycles of the Amazonian forests and pastures, *Nature*, *372*, 666–669, doi:10.1038/372666a0.

Nepstad, D. C., I. M. Tohver, D. Ray, P. Moutinho, and G. Cardinot (2007), Mortality of large trees and lianas following experimental drought in an Amazon forest, *Ecology*, *88*, 2259–2269, doi:10.1890/06-1046.1.

Ometto, J. P. H. B., A. D. Nobre, H. R. Rocha, P. Artaxo, and L. A. Martinelli (2005), Amazonia and the modern carbon cycle, *Oecologia*, *143*, 483–500.

Palace, M., M. Keller, G. P. Asner, J. N. M. Silva, and C. Passos (2007), Necromass in undisturbed and logged forests in the Brazilian Amazon, *For. Ecol. Manage.*, *23*, 309–318, doi:10.1016/j.foreco.2006.10.026.

Parotta, J. A., J. K. Francis, and R. R. DeAlmeida (1995), Trees of the Tapajós: A photographic field guide, *Gen. Tech. Rep. IITF-1*, U. S. Dep. of Agric., Rio Piedras, Puerto Rico.

Phillips, O. L., et al. (2002), Changes in growth of tropical forests: Evaluating potential biases, *Ecol. Appl.*, *12*, 576–587, doi:10.1890/1051-0761(2002)012[0576:CIGOTF]2.0.CO;2.

Prentice, I. C., G. D. Farquhar, M. J. R. Fasham, M. L. Goulden, M. Heimann, V. J. Jaramillo, H. S. Kheshgi, C. LeQuere, R. J. Scholes, and D. W. R. Wallace (2001), The carbon cycle and atmospheric carbon dioxide, in *Climate Change 2001: The Scientific Basis*, edited by J. T. Houghton et al., pp. 183–237, Cambridge Univ. Press, Cambridge, UK.

Rice, A. H., E. H. Pyle, S. R. Saleska, L. R. Hutyra, M. Palace, M. Keller, P. B. de Carmargo, K. Portilho, D. Marques, and S. C. Wofsy (2004), Carbon balance and vegetation dynamics in an old-growth Amazonian forest, *Ecol. Appl.*, *14*, 55–71, doi:10.1890/02-6006.

Saatchi, S. S., R. A. Houghton, R. C. S. Alvala, J. V. Soares, and Y. Yu (2007), Distribution of aboveground live biomass in the Amazon basin, *Global Change Biol.*, *13*, 816–837, doi:10.1111/j.1365-2486.2007.01323.x.

Saleska, S. R., et al. (2003), Carbon fluxes in old-growth Amazonian rainforest: Seasonality and disturbance-induced net carbon loss, *Science*, *302*, 1554–1557, doi:10.1126/science.1091165.

Saleska, S. R., K. Didan, A. R. Huete, and H. R. da Rocha (2007), Amazon forests green-up during 2005 drought, *Science*, *318*, 612, doi:10.1126/science.1146663.

Silver, W. L., J. Neff, M. McGroddy, E. Veldkamp, M. Keller, and R. Cosme (2000), Effects of soil texture on belowground carbon and nutrient storage in a lowland Amazonian forest ecosystem, *Ecosystems*, *3*, 193–209, doi:10.1007/s100210000019.

Summers, P. M. (1998), Estoque, decomposicão, e nutrients da liteira grossa em floresta de terra firme na Amazonia Central: Ciencias de florestas tropicais, Inst. Nac. de Pesquisas da Amazonia, Manaus, Brazil.

terSteege, H., et al. (2003), A spatial model of tree α-diversity and tree density for the Amazon, *Biodivers. Conserv.*, *12*, 2255–2277, doi:10.1023/A:1024593414624.

Van Wagner, C. E. (1968), Line intersect method in forest fuel sampling, *For. Sci.*, *14*, 20–26.

Vieira, S., et al. (2004), Forest structure and carbon dynamics in Amazonian tropical rain forest, *Oecologia*, *140*, 468–479, doi:10.1007/s00442-004-1598-z.

Vieira, S. A., S. E. Trumbore, P. B. Carmago, J. Q. Chambers, N. Higuchi, and L. A. Martinelli (2005), Slow growth rates of Amazonian trees: Consequences for carbon cycling, *Proc. Natl. Acad. Sci. U. S. A.*, *102*, 18,502–18,507, doi:10.1073/pnas.0505966102.

Williamson, G. B., W. F. Laurance, A. A. Oliveira, P. Delamonica, C. Gascon, T. E. Lovejoy, and L. Pohl (2000), Amazonian tree mortality during the 1997 El Nino drought, *Conserv. Biol.*, *14*, 1538–1542, doi:10.1046/j.1523-1739.2000.99298.x.

P. B. Carmago and S. Vieira, Universidade de Sao Paulo, Avenida Centenário 303, Piracicaba, SP 13416-000, Brazil.

V. Y. Chow, D. J. Curran, E. H. Pyle, G. W. Santoni, and S. C. Wofsy, Department of Earth and Planetary Sciences, Harvard University, Cambridge, MA 02138, USA. (pyle@fas.harvard.edu)

L. R. Hutyra, Urban Design and Planning, University of Washington, Seattle, WA 98195, USA.

W. F. Laurance and H. E. M. Nascimento, Biological Dynamics of Forest Fragments Project, National Institute for Amazonian Research, C.P. 478, Manaus, AM 69011-970, Brazil.

S. R. Saleska and J. van Haren, Department of Ecology and Evolutionary Biology, University of Arizona, Tuscon, AZ 85721, USA.